Quantification Methods for Clinical Studies in Nuclear Medicine - Applications in AMS, PET/CT and SPECT/CT

Sydoff, Marie

2013

Quantification Methods for Clinical Studies in Nuclear Medicine

Applications in AMS, PET/CT and SPECT/CT

Marie Sydoff

Medical Radiation Physics
Faculty of science, Lund University
2013

LUND
UNIVERSITY

AKADEMISK AVHANDLING

Som för avläggande av filosofie doktorsexamen vid Naturvetenskapliga fakulteten, Lunds Universitet, kommer att offentligen försvaras i lilla aulan, Jan Waldenströms gata 5, Skånes universitetssjukhus, Malmö, fredagen den 18 oktober 2013, kl. 9.00

Fakultetsopponent:

Prof. Peter Bernhardt, Avd. För Radiofysik, Inst. För kliniska vetenskaper, Sahlgrenska akademin, Göteborgs Universitet

Organization	Document name
LUND UNIVERSITY Department of Medical Radiation Physics Faculty of science	DOCTORAL DISSERTATION
	Date of issue October 18, 2013
Author(s)	Sponsoring organization
Marie Sydoff	

Title and subtitle

Quantification Methods for Clinical Studies in Nuclear Medicine – Applications in AMS, PET/CT and SPECT/CT

Abstract

An essential part of the development of new radiopharmaceuticals for use in diagnostic nuclear medicine is the determination of its biokinetic properties. The uptake and turn-over of the radiopharmaceutical in the source organs is of great interest since this could determine whether the radiopharmaceutical would be suitable for clinical use or not. It is also important that the biokinetics and dosimetry of the radiopharmaceuticals is thoroughly investigated in order to determine the radiation absorbed doses to various organs and tissues and the effective dose. This is done to evaluate the radiation risks in proportion to the benefits of their use. Modern imaging systems such as SPECT and PET have limitations that complicate the accurate estimation of activity content in source organs, and thus also the estimation of the radiation dose, to organs and tissues of the human body. As an example, the partial volume effect poses significant problems with the reliability of the activity values when imaging small volumes. Drawing regions of interest smaller than the actual structure could influence the results. With large ROIs, the activity concentration has been shown to be underestimated by 70 % for a 0.5-ml sphere and 31 % for a 20-ml sphere. With small ROIs the underestimation ranges from 66 to 16 % (Paper II). PET is becoming more common in radiotherapy treatment planning and can also be used to monitor treatment response. In these cases, as well as in planning of surgery, it is important that the volume of the structure of interest is quantified accurately. Using phantoms with fillable, hollow, plastic spheres with non-radioactive walls in an active background for estimation of the volume reproducing threshold would lead to overestimation of the tumour volume. The background dependence seen when using plastic phantoms is not present when using gelatin phantoms without radioactive walls (Paper III). As new imaging modalities are introduced, the measurement procedures and outline of clinical studies have to be adjusted to make use of the full potential of these new techniques. Biokinetic studies have commonly been performed using planar gamma camera images and the use of the conjugate view technique. As SPECT is very common at nuclear medicine clinics today, the use of this new and supposedly more accurate technique for determination of the biokinetics of radiopharmaceuticals is a natural step in the development process. It was shown that the organ dose estimations differed significantly when using complementary SPECT/CT measurements to quantify activity in the organs (i.e. to conduct dosimetry measurements) than when using planar images alone (Paper I). In drug development, AMS has become an important tool for quantifying the content of ^{14}C-labelled drug molecules in biological samples and to determine the pharmacokinetics of promising new drugs. PET or SPECT can be used simultaneously with AMS for analysis of the behaviour of the same compound labelled with positron (PET) or photon (SPECT) emitting radionuclides. The information acquired from the different modalities is complementary i.e. AMS gives information about the pharmacokinetic profile in blood and urine and PET and SPECT gives information about the pharmacokinetic behaviour in organs and tissues. The human microdosing concept is aiming to speed up drug development and reducing the costs by improved candidate selection in early drug development. In order to promote the use AMS for analysis of biomedical samples, a fast and easily implemented sample preparation method is needed, which converts the biological samples to solid graphite. The precision of such a method is lower that earlier more time-consuming methods, but it is well suited for this type of application (Paper IV). In order to facilitate the implementation of the AMS technique closer to the clinics, the development of smaller AMS systems is a constantly ongoing process. When comparing high-voltage AMS with low-voltage AMS it is shown that the AMS instruments themselves were comparable and that low voltage AMS provides an excellent alternative to the larger and more expensive high-voltage tandem AMS systems (Paper V).

Key words: AMS, PET, SPECT, quantification, biokinetics, pharmacokinetics, microdosing

Classification system and/or index terms (if any)

Supplementary bibliographical information		Language: English
ISSN and key title		ISBN 978-91-7473-675-5
Recipient's notes	Number of pages	Price
	Security classification	

Signature _____ Date _____

Quantification Methods for Clinical Studies in Nuclear Medicine

Applications in AMS, PET/CT and SPECT/CT

Marie Sydoff

Medical Radiation Physics
Faculty of science, Lund University
2013

LUND
UNIVERSITY

marie@sydoff.se

Medical Radiation Physics,
Faculty of science,
Lund University

ISBN 978-91-7473-675-5 (tryckt)
ISBN 978-91-7473-676-2 (pdf)

Printed in Sweden by Media-Tryck, Lund University
Lund 2013

"Adventure is the result of poor planning."
/Colonel Blatchford Snell

Abstract

An essential part of the development of new radiopharmaceuticals for use in diagnostic nuclear medicine is the determination of its biokinetic properties. The uptake and turn-over of the radiopharmaceutical in the source organs is of great interest since this could determine whether the radiopharmaceutical would be suitable for clinical use or not. It is also important that the biokinetics and dosimetry of the radiopharmaceuticals is thoroughly investigated in order to determine the radiation absorbed doses to various organs and tissues and the effective dose. This is done to evaluate the radiation risks, which is one of the risks factors that have to be compared, with the benefits of their use.

Modern imaging systems such as single photon emission computed tomography (SPECT) and positron emission tomography (PET) have limitations that complicate the accurate estimation of the activity content in source organs, and thus also the estimation of the radiation absorbed dose, to organs and tissues of the human body. As an example, the partial volume effect poses significant problems with the reliability of the activity values when imaging small volumes. Drawing regions of interest smaller than the actual structure could influence the results. With large ROIs, the activity concentration has been shown to be underestimated by 70 % for a 0.5-ml sphere and 31 % for a 20-ml sphere. With small ROIs the underestimation ranges from 66 to 16 % (Paper II).

PET is becoming more common in radiotherapy treatment planning and also used to monitor treatment response. In these cases, as well as in planning of surgery, it is important that the volume of the structure of interest is estimated accurately. Using phantoms with fillable, hollow, plastic spheres in an active background for estimation of the volume reproducing threshold would lead to overestimation of the tumour volume. The background dependence seen when using plastic phantoms is not present when using gelatin phantoms without walls (Paper III).

As new imaging modalities are introduced, the measurement procedures and outline of clinical studies have to be adjusted to make use of the full potential of these new techniques. Biokinetic studies have commonly been performed using planar gamma camera images and the use of the conjugate view technique. As SPECT is very common at nuclear medicine clinics today, the use of this new and supposedly more accurate technique

for determination of the biokinetics of radiopharmaceuticals is a natural step in the development process. It was shown that the organ dose estimations differed significantly when using complementary SPECT/CT measurements to quantify activity in the organs (i.e. to conduct dosimetry measurements) than when using planar images alone (Paper I).

In drug development, accelerator mass spectrometry (AMS) has become an important tool for quantifying the content of ^{14}C-labelled drug molecules in biological samples and to determine the pharmacokinetics of promising new drugs. PET or SPECT can be used simultaneously with AMS for analysis of the behaviour of the same compound labelled with positron (PET) or photon (SPECT) emitting radionuclides. The information acquired from the different modalities is complementary i.e. AMS gives information about the pharmacokinetic profile in blood and urine and PET and SPECT gives information about the pharmacokinetic behaviour in organs and tissues.

The human microdosing concept is aiming to speed up drug development and reducing the costs by improved candidate selection in early drug development. In order to promote the use of AMS for analysis of biomedical samples, a fast and easily implemented sample preparation method is needed, which converts the biological samples to solid graphite. The precision of such a method, which is developed in Paper IV, is lower that earlier more time-consuming methods, but it is well suited for this type of application.

In order to facilitate the implementation of the AMS technique closer to the clinics, the development of smaller AMS systems is a constantly ongoing process. When comparing high-voltage AMS with low-voltage AMS it is shown that the AMS instruments themselves were comparable and that low voltage AMS provides a good alternative to the larger and more expensive high-voltage tandem AMS systems (Paper V).

Summary in Swedish

Inom området diagnostisk nuklearmedicin används radioaktiva läkemedel som ges (administreras) till patienterna i syfte att diagnostisera ett antal olika sjukdomstillstånd. Då man tar fram nya radioaktiva läkemedel för användning inom diagnostisk nuklearmedicin handlar det många gånger om att uppskatta mängden av ett visst upptag av radiofarmakat i olika organ och vävnader i kroppen. Man kan då få en uppfattning om hur ämnet fördelas i kroppen och hur länge det dröjer sig kvar i olika organ och vävnader. Man studerar ämnets väg genom kroppen, den tid det tar för ämnet att tas upp eller att utsöndras, vilket kan ge värdefull information om den fortsatta användningen av detta läkemedel. Inom bilddiagnostiken vill man att kontrasten mellan sjuk och frisk vävnad ska bli hög för att lättare kunna ställa diagnos. Något som man självklart också måste ta hänsyn till är att patienten inte ska utsättas för onödigt mycket strålning från det radioaktiva ämnet. Detta kan man fastställa genom att mäta hur mycket av det radioaktiva ämnet som tagits upp i kroppens olika organ samt i blod och urin vid olika tidpunkter efter tillförseln av det radioaktiva läkemedlet. Mätningarna görs med de olika kameror som används inom diagnostiken, såsom SPECT (single photon emission computed tomography) eller PET (positron emission tomography) som mäter den strålning som skickas ut från det radioaktiva ämnet som man har gett till patienten och gör om detta till en tredimensionell bild av ämnets fördelning i kroppen. För att få en korrekt uppskattning av stråldosen från det radioaktiva ämnet är det då viktigt att använda sig av metoder som ”översätter” informationen i dessa bilder till innehållet av det radioaktiva ämnet i olika organ och vävnader.

PET och SPECT-kamerorna kan även användas för att uppskatta storleken av exempelvis cancertumörer inför eller under pågående cytostatikabehandling eller strålbehandling. En förändring av tumörstorleken kan då visa hur effektiv en behandling är. Vid planering inför strålbehandling är det mycket viktigt att kunna bestämma tumörens storlek samt läge noggrant eftersom dessa ligger till grund för beslutet om hur stor volym som skall bestrålas. Ju större volym som inkluderas runt tumören, desto mer strålning utsätts den friska vävnaden för. För att minimera risken för detta behöver man även här arbeta fram metoder som kvantifierar bilddata på ett så korrekt sätt som möjligt.

En ”icke bildgivande” metod som fått stor spridning inom klinisk forskning när det gäller läkemedelsutveckling är acceleratorbaserad mass spektrometri (AMS) där man analyserar atominnehållet i biologiska prover. Den vanligaste tillämpningen för AMS är datering av arkeologiska och geologiska prover med hjälp av kol-14-metoden, men denna teknik kan även användas för studier av hur läkemedel fördelas, tas upp och utsöndras. Man märker läkemedelssubstansen med radioaktivt kol-14 och tillför mycket små mängder (sk. mikrodoser) av den märkta substansen till försökspersoner. Man mäter sedan innehållet av kol-14 i prover av blod och urin som samlats in vid olika tidpunkter efter att man injicerat läkemedlet. Man kan även använda de ”bildgivande” metoderna PET och SPECT för att studera fördelningen av läkemedel i organen men då måste man märka läkemedlen med andra typer av radioaktiva ämnen som går att mäta med dessa utrustningar. Fördelen med att ge mikrodoser till försökspersonerna är att man använder så små mängder av läkemedel att det är möjligt att utföra tester på människor mycket tidigare i processen än med traditionella metoder. Man har då möjlighet att korta ner tiden för utveckling av nya läkemedel genom att sortera ut dåliga läkemedelskandidater redan efter dessa tester.

AMS är en mycket noggrann mätmetod med vilken man kan räkna enskilda atomer. Man kan dock se skillnader i resultat vid användning av olika typer av acceleratorer eller vid användning av olika metoder för att förbereda de prover som ska analyseras. Det är därför viktigt att undersöka vilka skillnader detta kan ge upphov till för att kunna göra en korrekt uppskattning av läkemedelskoncentrationen i blod och urin.

Utvecklingen av system, både ”bildgivande” och ”icke bildgivande”, går ständigt framåt. För att kunna utnyttja den fulla potentialen av dessa system och känna sig trygg med att använda dem i kliniska studier samt vid diagnostik, krävs ett ständigt arbete och en vidareutveckling av befintliga metoder. De metoder som beskrivs i denna avhandling är ett bidrag till detta.

Abbreviations

AMS	Accelerator Mass Spectrometry
CT	Computed Tomography
CREAM	Consortium for Resourcing and Evaluating AMS
DAT	Dopamine Transporter
DEW	Double Energy Window
DLB	Dementia with Lewy Bodies
EMEA	European Medicines Agency
EUMAPP	European Union Microdose AMS Partnership Program
FDA	United States Food and Drug Administration
FDG	Fluoro Deoxy Glucose
FP-CIT	N-ω-fluoropropyl-2β-carbomethoxy-3β-[4-iodophenyl]nortropane
FWHM	Full Width at Half Maximum
LLI	Lower Large Intestine
LSC	Liquid Scintillation Counting
MIRD	Committee on Medical Internal Radiation Dose
MISO	Fluoromisonidazol
MRI	Magnetic Resonance Imaging
OLINDA	Organ Level Internal Dose Assessment (Computer software)
PET	Positron Emission Tomography
pMC	percent Modern Carbon
PVE	Partial Volume Effect
ROI	Region Of Interest
SAAM	Simulation Analysis And Modeling (Computer software)
SERT	Serotonin Transporter
SI	Small Intestine
SPECT	Single Photon Emission Computed Tomography
SSAMS	Single Stage Accelerator Mass Spectrometry
SSRI	Selective Serotonin Reuptake Inhibitor
TEW	Triple Energy Window
ULI	Upper Large Intestine

Original papers

This thesis is based on the following publications, which will be referred to in the text by their roman numerals.

I. *Determination of the biodistribution and dosimetry of ^{123}I-FP-CIT in male patients with suspected Parkinsonism or Lewy body dementia using planar and combined planar and SPECT/CT imaging*
Sydoff M, Lizana H, Mattsson S, Stabin M G, Leide-Svegborn S
Accepted for publication in: Appl Radiat Isotopes

II. *Absolute quantification of activity content from PET images using the Philips Gemini TF PET/CT system*
Sydoff M, Uusijärvi H, Leide-Svegborn S, Mattsson S
Radiat Prot Dosim, 2010; 139(1-3): 236-9

III. *Use of wall-less ^{18}F-doped gelatin phantoms for improved volume delineation and quantification in PET/CT*
Sydoff M, Andersson M, Mattsson S, Leide-Svegborn S
Submitted for publication in: Phys Med Biol

IV. *^{14}C sample preparation for AMS microdosing studies at Lund University using online combustion and septa-sealed vials*
Sydoff M, Stenström K
Nucl Instrum Meth B. 2009; 268: 924-926

V. *Evaluation of a high-throughput graphitization system and low-voltage AMS for analysis of biomedical samples for microdosing studies*
Sydoff M, Stenström K
Submitted for publication in: Rapid Commun Mass Sp

Preliminary reports

Preliminary reports have been presented at the following international meetings and conferences:

i. *Biokinetics and dosimetry of ^{123}I-FP-CIT*
Giussani A, Sydoff M, Leide-Svegborn S, Mattsson S, Uusijärvi-Lizana H, Tavola F, Veronese I, Cantone M-C, Zankl M, Hoeschen Ch
11th International Conference on the Health Effects of Incorporated Radionuclides (HEIR), Berkeley, CA, October 2013

ii. *A biokinetic and dosimetric model for ^{123}I-ioflupane*
Tavola F, Veronese I, Cantone M-C, Sydoff M, Leide-Svegborn S, Mattsson S, Uusijärvi-Lizana H, Giussani A
EANM'12, Milan, Italy 2012

iii. *Biokinetics and dosimetry of DaTSCAN™ ioflupane (^{123}I) in patients with suspected Parkinsonism or Lewy body dementia*
Sydoff M, Lizana H, Leide-Svegborn S, Mattsson S
EANM'11, Birmingham, England 2011

iv. *Absolute quantification of activity content in PET images using the Philips Gemini TF PET/CT system*
Sydoff M, Uusijärvi H, Leide-Svegborn S, Mattsson S
Third Malmö conference in medical imaging, Malmö, Sweden, June 2009

v. *Microdosing for early biokinetic studies in man*
Stenström K, Sydoff M, Mattsson S
Third Malmö conference in medical imaging, Malmö, Sweden, June 2009

vi. *Experiences from the production of an AMS ^{14}C sucrose standard for high-activity measurements*
Sydoff M, Stenström K
20th International Radiocarbon conference, Kona, Hawaii, May 2009

vii. *Development of a simplified graphitization method based on online-combustion of biological samples for the conversion of CO_2 to AMS graphite targets with septa-sealed vials*
Sydoff M, Stenström K
11th International Conference on Accelerator Mass Spectrometry, Rome, Italy, September 2008.

viii. *Development of an improved method for analysis of biological samples with small-scale AMS and a simplified graphitization process*
Sydoff M, Stenström K
EUFEPS Conference on Optimising Drug Discovery and Development, Basel, Switzerland, December 2007

ix. *Activity quantification of planar gamma camera images*
Leide Svegborn S, Sydoff M, Norrgren K
EANM'06, Athens, Greece, October 2006

x. *Quantification of activity concentration in vivo using planar gamma camera images*
Sydoff M, Norrgren K, Leide-Svegborn S
International Conference on Radiation Interaction with Material and its use in Technologies, Kaunas, Lithuania, September 2006

Other related publications by the author

- *A compartmental model for biokinetics and dosimetry of ^{18}F-Choline in prostate cancer patients*
  Giussani A, Janzen T, Uusijärvi-Lizana H, Tavola F, Zankl M, Sydoff M, Bjartell A, Leide-Svegborn S, Söderberg M, Mattsson S, Hoeschen Ch, Cantone M-C
  J Nucl Med 2012; 53:985–993

- *Microdosing for early biokinetic studies in humans*
  Stenström K, Sydoff M, Mattsson S
  Radiat Prot Dosim, 2010; 139(1-3): 348-52

- *Experiences of production and homogeneity analysis of an AMS ^{14}C sucrose standard for high-activity measurements*
  Sydoff M, Stenström K
  Radiocarbon, 2010; 52 (2–3): 1351–1357

- *Optimising PET/CT and SPECT/CT investigations. The MADEIRA project*
  Uusijärvi H, Sydoff M, Söderberg M, Leide-Svegborn S, Mattsson S
  Proc 6th International Conference on Medical Physics in the Baltic States 2008: 49-51

Contents

Introduction 17
Objectives 21
Quantification 23
Sources of image degradation 23
Planar quantification 24
Attenuation correction 25
Scatter correction 26
Background activity correction 26
Quantification in SPECT/CT 27
Attenuation correction 28
Scatter correction 28
SPECT/CT in dosimetry 28
Quantification in PET/CT 29
Partial volume effect in PET/CT 30
ROI definition 32
Volume quantification 34
Phantom development 35
Threshold-based volume delineation 37
Influence of phantom walls 40
Biokinetic studies 43
Internal dosimetry 44
Outline of a biokinetic study 46
Biokinetic modeling 48
Microdosing 53
Sample preparation 56
AMS analysis 59
High vs. low voltage AMS 60
Conclusions 67
Acknowledgements 69
References 71

Introduction

An essential part of the development of new radiopharmaceuticals for use in diagnostic nuclear medicine is the determination of its biokinetic properties. The retention and turn-over of the radiopharmaceutical in the source organs is of great interest since this could determine whether the radiopharmaceutical would be suitable for clinical use or not and also to evaluate the radiation risks, which is one of the risks factors that have to be compared with the benefits of their use. The biokinetics of the radiopharmaceuticals used should be thoroughly investigated in order to determine the absorbed doses to various organs and tissues and the effective dose. Accordingly, it is important that the biokinetic behaviour be thoroughly investigated not only in healthy volunteers, but also in patients in order to estimate the influence of medication on the radiotracer uptake and its biokinetics and dosimetry. For example, the use of selective serotonin reuptake inhibitors (SSRIs) leads to a striatal uptake increase of approximately 10%, and ^{123}I-FP-CIT binds to the serotonin transporter (SERT), which is expressed extensively in the lungs (Booij *et al.*, 2007). This could possibly influence the uptake and thus the absorbed dose to the lungs.

As new imaging modalities are introduced, the measurement procedures and outline of clinical studies have to be adjusted to make use of the full potential of these new techniques. Biokinetic studies regarding photon emitting radionuclides have since long time been performed using planar gamma camera images and the use of the conjugate view technique. Data from human imaging provide a good estimate of the absorbed doses by different organs and tissues as well as the effective dose, but there are limitations involving the quantification of organ activity content from planar images.

Activity quantification using planar gamma camera images is a time-consuming process, requiring methods that correct for attenuation, scatter, background activity and organ and body thickness. Quantification with tomographic imaging has also been shown to be superior to that with planar imaging (Pereira *et al.*, 2010) and since SPECT is very common at nuclear medicine clinics today, the use of this new and supposedly more accurate technique for determination of the biokinetics of radiopharmaceuticals is a natural step in the development process. The use of complementary SPECT/CT measurements to quantify activity in the

organs is one way of reducing the effect of several of the image-degrading parameters seen in planar gamma camera images. However, SPECT measurements are more challenging for the patients and an examination is somewhat more time-consuming than an examination based on planar imaging. The quantification can thus be based on the activity seen in the SPECT/CT images, and the shape of the time-activity curve can be based on planar images. In Paper I the biodistribution and dosimetry of ^{123}I-FP-CIT in adult male patients was determined comparing dosimetry results from quantification of activity from planar gamma camera imaging alone or with the use of complementary SPECT/CT imaging.

Modern imaging systems such as SPECT and PET have limitations that complicate the accurate estimation of activity content in source organs, and thus the estimation of the radiation dose, to organs and tissues of the human body. As an example, the partial volume effect (PVE) poses significant problems with the recovery of true activity of small volumes (Hoffman *et al.*, 1979).

The PVE is an effect originating from the poor spatial resolution of the cameras (typically 5-7mm full width at half maximum; FWHM). The PVE results in spread of signal into neighbouring pixels, both from a high uptake into the background (spill-out) or the reverse (spill-in). Several different methods for the correction of PVE has been developed over the years, both image-based and reconstruction-based (Aston *et al.*, 2002; Geworski *et al.*, 2000; Soret *et al.*, 2007) but since different imaging systems differ somewhat in regard to e.g. spatial resolution and sensitivity, the methods often need to be adjusted to the type of PET system being investigated. In Paper II the influence of region of interest (ROI) size and a simple PVE correction method was investigated for a Philips Gemini TF PET/CT system.

PET is becoming more common in radiotherapy treatment planning and is also a valuable tool for staging a variety of different diseases and for evaluating the treatment response of many different types of tumours, i.e., non-small cell lung cancer (NSCLC) (Higashi *et al.*, 2002) and head-and-neck cancer (Daisne *et al.*, 2004). The uptake of ^{18}F-FDG, which is the most commonly used PET radiopharmaceutical, correlates well with tumour grade and patient prognosis (Vesselle *et al.*, 2000). Bradley et al. showed that in radiation therapy, the estimated target volume changed in 50% of the cases when PET/CT was used for volume estimation, compared to cases using only CT (Bradley *et al.*, 2004). To spare healthy tissue in radiotherapy, for planning of surgery and to evaluate treatment response correctly makes it important that the volume of the imaged structure is quantified accurately. In Paper III a phantom without walls was developed for use in volume quantification. A volume delineation method was used to estimate the influence of the phantom walls.

Accelerator mass spectrometry (AMS) was for the first time suggested as a tool to obtain pharmacokinetic data from clinical studies in 1978 (Keilson and Waterhouse, 1978). Today, AMS has become an important tool for quantifying the ^{14}C content in biological samples from microdosing studies to determine the pharmacokinetics of promising new drugs. Other modalities, such as PET or SPECT can be used simultaneously with AMS for analysis of the behaviour of the same compound labelled with positron (PET; ^{18}F) or photon (SPECT; ^{99m}Tc, ^{123}I, etcetera) emitting radionuclides. The information acquired from the different modalities is complementary i.e. AMS yields information about the pharmacokinetic profile in blood and urine and PET and SPECT present information about the retention and turnover of the radiopharmaceutical in organs and tissues.

The human microdosing concept is aiming to speed up drug development and reducing the costs by improved candidate selection in early drug development (Garner and Lappin, 2006; Stenström *et al.*, 2010). The alternatives to AMS in early drug development is the use of animal testing or *in silico* modelling, but in one of five cases, the predictions made from animal testing does not correlate with the behaviour in humans. This makes the first in man testing more challenging since some of the metabolic differences between animals and humans could lead to rejection of new drugs after a long time of animal and toxicology testing. The introduction of a human "Phase 0"-stage, using sub-pharmacological doses early in the development process, could lower the rejection rate of new drugs and thus make new drugs reach the market faster and to more reasonable prices.

In order to promote the use of AMS for analysis of biomedical samples from microdosing studies, a fast and easily implemented sample preparation method is needed, which converts the biological samples to solid graphite. This method was developed in Paper IV. The conversion is done by combustion of samples and collection of the carbon dioxide formed in the process. The carbon dioxide is then reduced over an iron catalyst to graphite, which is pressed into aluminium cathodes and used as AMS targets. Graphitization can be done in several ways depending on the need for high precision, short preparation time or easy handling (Vogel, 1992; Ognibene *et al.*, 2003; Getachew *et al.*, 2006; Xu *et al.*, 2007; Sydoff and Stenström, 2010). There is a trade-off between these parameters depending on the chosen method, thus the precision of the high-throughput method is somewhat lower than the earlier, more time-consuming methods but it is quite sufficient for analysis of biological samples from microdosing studies.

In implementation of the AMS technique closer to the clinics, the development of compact, easy-to-operate, commercially available AMS instruments is a constantly ongoing process (Synal *et al.*, 2007; Skog *et al.*, 2010; Wacker *et al.*, 2010). Conventional AMS systems operate at

accelerator voltages in the 5-6 MV range whereas the compact systems operate in the 200 – 500 kV range. The lower voltage makes the system easier to handle and the design of the acceleration tube makes the system smaller, thus it can be housed directly at the pharmaceutical and biomedical companies. In Paper V a low and a high voltage AMS system were compared to investigate whether the systems are comparable and if the high-throughput graphitization system (developed in paper IV) is suitable for use in measurements of biomedical samples from microdosing studies.

Objectives

The overall objective of this work was to develop methods for *in vivo* quantification of parameters such as activity and volume and for ultra-low concentrations of ^{14}C in samples of urine and blood, for applications in SPECT/CT, PET/CT and AMS. The detailed objectives were:

- To determine the biodistribution and dosimetry of ^{123}I-FP-CIT in adult male patients, comparing dosimetry results from quantification of activity from planar gamma camera imaging alone or in combination with SPECT/CT imaging (Paper I).
- To evaluate the reliability of activity concentration values given by the Philips Gemini TF PET/CT system and the influence of ROI size and structure size on the quantification of activity (Paper II).
- To develop a phantom without walls for volume delineation and quantification in PET and to study the influence of the sphere walls in regular phantoms (Paper III).
- To develop and evaluate a simplified method for the conversion of biological samples to solid graphite for ^{14}C analysis of biological samples from microdosing studies (Paper IV).
- To compare a low and a high voltage AMS system to investigate whether the low voltage system is comparable with the high voltage system and if the high-throughput graphitization system (developed in paper IV) is suitable for use in measuring biomedical samples from microdosing studies (Paper V).

Quantification

To reliably estimate the prognosis and treatment response of a wide range of diseases, as well as the absorbed dose and the effective dose following a nuclear medicine diagnostic procedure, it is essential that the quantification of the activity concentration in the organs and tissues is correctly done. Absolute quantification of the activity content can be done by imaging the retention and distribution of a radiopharmaceutical in the human body using different imaging systems such as gamma camera, SPECT/CT and PET/CT systems. To derive information on the retention and distribution of the radiopharmaceutical, the image pixel values have to be converted into activity concentrations. Effects related to attenuation, scatter, patient and organ motion, spatial resolution and sensitivity of the imaging systems are all factors contributing to the non-linearity of this conversion. The quantification is also highly dependent on the chosen image reconstruction method, measurement procedure and acquisition parameters, and thus this must be considered when quantifying the concentration of the chosen radionuclide for diagnostic and dosimetric purposes.

The development of the imaging systems have been extensive from the first Anger cameras invented in the late 1950s (Anger, 1958) to the first rotating scintillation cameras in the late 1960s (Anger *et al.*, 1967) and the first PET ring detector systems in the mid-seventies (Derenzo *et al.*, 1975) to today's state-of-the-art tomographic imaging systems combining different modalities such as SPECT/CT, PET/CT and PET/MRI. The continuous development of new imaging systems requires a constantly ongoing optimisation of current methods to be confident to know that the systems can be used for correct diagnosis of a variety of different diseases and in the development of new radiopharmaceuticals.

Sources of image degradation

In nuclear medicine imaging there are several sources of degradation affecting the images. The main limitations of accuracy in the quantification of activity from nuclear medicine images are: attenuation, scatter and the presence of activity in overlying and underlying tissue. However, the

sensitivity and spatial resolution of the imaging system sets the systems ultimate limit of accuracy. Other limitations are user-dependent and include the manual drawing of regions of interest (ROIs) which can make estimations to differ a great deal depending on experience and matter of opinion in drawing the ROIs.

Planar quantification

Some of the first studies on the absolute measurement of activity in organs in which the geometric mean method is presented and evaluated are the studies of Thomas *et al.* (1976) and Fleming (1979). The method is also commonly referred to as the conjugate view method. This method is still used today and gives good estimate of the activity content in organs and tissues from planar images. The geometric mean method comprises the use of two conjugate (anterior and posterior) whole body scans and takes the organ and body thickness into account, and theoretically the results are independent of the source depth. However, the projection images have the disadvantage of projecting all structures in one plane, which leads to difficulties in estimation of the activity content in overlapping structures.

The source activity A_j can be calculated using the following expression (Thomas *et al.*, 1976):

$$A_j = \sqrt{\frac{N_A N_P}{e^{-\mu_e T_j}}} \frac{f_j}{C} \qquad \text{Eq. 1}$$

$$f_j = \frac{\mu_j t_j / 2}{sinh(\mu_j t_j / 2)} \qquad \text{Eq. 2}$$

N_A and N_P are the count rate (counts per second, cps) as calculated from the anterior and posterior images, C is the system calibration factor in cps/MBq, t_j is the organ thickness and T_j is the body thickness at the placement of the organ ROI. μ_j is the linear attenuation coefficient in an organ with thickness t_j, and μ_e is the effective attenuation coefficient.

The anterior and posterior count rates are estimated from the planar images by drawing ROIs delineating the organs of interest. The number of counts in the anterior and posterior ROIs is then corrected for attenuation, scatter and background activity i.e. activity in overlying and underlying tissue. A common approach to reduce the effect of overlapping tissue (assuming a uniform uptake) is that smaller ROIs can be drawn in the different organs and the counts/pixel values multiplied by the number of pixels that were estimated for the whole organ (Sjögreen *et al.*, 2002; Van de Wiele *et al.*, 2001; Jönsson *et al.*, 2005). For paired organs, such as the lungs and kidneys, an ROI can be drawn over the organ that is most visible and thus the least affected by overlapping tissue.

Using only planar imaging, the estimation of the organ and body thickness is not very accurate and could result in large uncertainties due to patient variability (Leide-Svegborn, 1999). However, the use of CT as a tool in estimating organ and body thickness, and also the location of the organs, could reduce the uncertainties.

Attenuation correction

A major impact on image degradation, together with photon scattering, is the attenuation of photons in the body of a patient before exiting it and reaching the detector. Without compensation for attenuated photons, an image of a source distribution would deviate substantially from the true distribution. When imaging a homogeneous source distribution, the activity would appear higher in structures closer to the surface of the body. This is due to the longer path that the photons have to travel and thus the higher risk of interaction before leaving the body. Attenuation compensation in planar imaging is usually made by the acquisition of a transmission image. Commonly, a ^{57}Co flood source is placed on one side of the patient/phantom and the transmitted photons are detected on the other side. An additional image of the flood source is also acquired in absence of the patient/phantom. Similar ROIs are then drawn in the transmission images and the difference in the count rates are a measure of the attenuation in the patient/phantom (Norrgren *et al.*, 2003).

Today, when hybrid scanners become more and more common, the CT incorporated in the scanner can be used to make attenuation maps of the patients by converting Hounsfield units from CT images to linear attenuation coefficients (Brown *et al.*, 2008; Bai *et al.*, 2003; Mattsson and Skretting, 2011). A method utilizing the so-called scout view, which is an x-ray image acquired before the CT measurement for positioning reasons, to construct attenuation maps of the imaged patient has been developed (Minarik *et al.*, 2005).

Scatter correction

Another image degradation factor is the scattering of photons within the imaged body, which contributes to the blurring of the image. The number and energy distribution of scattered photons depends on the attenuation properties of the imaged body and also the distribution of the radionuclide in the body. Photons that have been scattered by Compton scattering are deflected from its original path and are less energetic than the original photons, thus this effect could be reduced by accepting only photons that fall within the range of a small, preset energy interval centered around the full-absorption peak. Scatter is however not completely eliminated by this approach due to the low energy resolution and the presence of scattered photons in the full-absorption peak window.

Scatter compensation can be made by estimation of the number of photons that fall outside the full-absorption peak energy window in the energy spectrum of the radionuclide used. Estimations of the number of scattered photons are made in energy windows with a certain width placed adjacent to the full-absorption peak window. The most commonly used energy-based methods are the dual energy window method (DEW) and the triple energy window method (TEW). The DEW method includes an energy window on the lower side of the full-absorption peak window and the TEW method uses two narrow energy windows placed on either side of the full-absorption peak window and in which the number of scattered photons is estimated as the number of counts present under the curve defining the energy spectrum (King *et al.*, 1992; Dewaraja *et al.*, 1998). The number of scattered photons in the sub-windows is then subtracted from the number of photons in the full-absorption peak window.

Background activity correction

Correction for activity in over- and underlying tissue i.e. in the background of planar images can be done in a variety of ways, and the three most common approaches are the so-called Gates, Kojima and Bujis background correction methods (Gates, 1983; Kojima *et al.*, 1993; Buijs *et al.*, 1998). Gates' method is also referred to as the conventional background correction method and is the simplest method, assuming a uniform background. Background ROIs are drawn in the vicinity of the organ of interest and the count rate in the background ROI is subtracted from the organ ROI. This method is easy to apply, but makes an overestimation of the background activity, since the thickness of the organ is not considered. The Kojima method does take the organ thickness into account, and also the organ depth. This is a method that gives more accurate results than the Gates method but has a somewhat more complicated approach. A correction factor including the organ and body thickness, the distance

between the anterior surface of the body and the anterior organ surface, and the distance between the posterior surface of the body and the anterior organ surface is applied to the background count rate. Bujis background correction method is somewhat simpler than the Kojima method and does not require information of the organ depth. However, it has been shown to give more accurate results than the Gates method and results comparable with the ones achieved with the Kojima method (Buijs *et al.*, 1998). In paper 1, background correction is performed using a correction factor that considers the organ thickness t_j and the body thickness T_j:

$$N_{A,P} = N'_{A,P} - N_{bgr} \cdot F, \text{ where } F = 1 - \left(\frac{t_j}{T_j}\right) \quad \text{Eq. 3}$$

In these equations, $N_{A,P}$ is the background-corrected count rate in either the anterior or posterior image, and $N'_{A,P}$ is the uncorrected count rate. The organ and body thicknesses were measured in the CT images with a precision of approximately ± 3 mm, which makes the estimations much more accurate than former methods with the use of lateral, planar images for organ and body thickness estimations.

Quantification in SPECT/CT

SPECT imaging data is gathered by letting one or more gamma camera detectors revolve around the patient, acquiring planar images from several different angles of the patient. Reconstruction of projection images result in 3D images with the advantage of separating interesting structures and making the volume and activity estimation more accurate. Since SPECT imaging diminishes problems with over- and underlying activity the quantification using SPECT has been shown to be superior to that with planar imaging (Keyes *et al.*, 1977; Jaszczak *et al.*, 1977; Savolainen, 1992; Pereira *et al.*, 2010). The accuracy of activity and volume quantification is however influenced by several other degrading factors. The main sources of degradation in SPECT images are attenuation, scatter, system resolution and patient motion but reconstruction of images can also affect the result of the activity quantification. In the diagnosis of neurodegenerative disorders as Parkinson's disease, Alzheimer's disease or dementia with Lewy bodies (DLB), imaged using the radiopharmaceutical ^{123}I-FP-CIT the number of iterations and subsets has an influence on the assessment of striatal uptake (Dickson *et al.*, 2010; Söderberg *et al.*, 2012). Absolute activity quantification could be useful in assessment of disease progression and thus the choice of reconstruction method becomes essential (Booij *et al.*, 2001).

Attenuation correction

The integration of SPECT and CT into hybrid SPECT/CT scanners provides significant advantages in attenuation correction. Attenuation compensation is made with a co-registered 3D attenuation map obtained by the CT incorporated in the SPECT/CT scanner. The attenuation map is generated by converting HU values in the CT image volume into a patient-specific attenuation map (Brown *et al.*, 2008; Bai *et al.*, 2003). The CT image is also valuable in order to produce fusion images for enhanced visualization and anatomic localization of activity uptake in e.g. tumours in radiotherapy treatment planning.

Scatter correction

Since the SPECT image data consist of data from a number of projection images, reconstructed to produce a 3D image, scatter compensation in SPECT can be made similar to the scatter correction in planar imaging. The TEW scatter correction method is commonly used, by the co-registration of counts in energy windows adjacent to the full-absorption peak window. The attenuation map obtained by the CT can however be used for scatter correction and methods for this have been developed by a number of groups, but a golden standard for scatter correction in SPECT is yet to be implemented on commercial systems (Hutton *et al.*, 2011; Mukai *et al.*, 1988; Larsson *et al.*, 2003).

SPECT/CT in dosimetry

SPECT data can be used for rescaling time-activity-curves from planar images to get the ease and speed of planar imaging and the accuracy of SPECT imaging (He 2006, 2009). This was done in Paper I in which the absolute quantification of activity of ^{123}I-FP-CIT was based on the activity seen in the SPECT/CT images, and the shape of the time-activity curve was based on the planar images. The advantage of SPECT/CT imaging in comparison with planar imaging is an increased accuracy, but the drawbacks are the longer measurement time and the higher dose received by the subjects due to the CT measurement. A combination of these approaches, employed in Paper I, make use of the advantages of both methodologies.

Quantification in PET/CT

The number of PET/CT systems operational in clinical routine has increased widely during the last decade. It is a valuable tool for staging, treatment planning, and evaluation of treatment response for many different types of tumours i.e. non-small cell lung cancer (NSCLC) (Higashi *et al.*, 2002) and head-and-neck cancer (Daisne *et al.*, 2004). Quantitative results from the PET/CT scanner can also be used for investigations regarding neurodegenerative diseases, such as Alzheimer's and Parkinson's disease, in the calculation of absorbed doses and effective dose in development of new radiopharmaceuticals and in the estimation of the potential risks in undergoing a diagnostic procedure.

The most common radiopharmaceutical used in PET/CT imaging is the positron emitting glucose analogue ^{18}F-fluoro-2-deoxy-D-glucose (FDG). The uptake of ^{18}F-FDG has been shown to correlate well with tumour grade and prognosis (Vesselle *et al.*, 2000) and it is thus widely used in oncology for localization and diagnosis of a number of tumour diseases such as e.g. small-cell and non-small cell lung cancer and breast cancer, etc. (Caldwell *et al.*, 2001; Krak *et al.*, 2004; Pandit *et al.*, 2003). One thing worth considering is that inflammatory processes also have an increased glucose metabolism, thus FDG is not tumour specific. Other PET radiopharmaceuticals may have a higher specificity than ^{18}F-FDG, but ^{18}F-FDG is the most common radiopharmaceutical in PET imaging and the specificity of PET/CT in tumour assessment is higher than the use of only CT. ^{18}F-choline, for example, is used for preoperative staging and assessment of bone metastases as well as post-operative investigation of lymph node metastases in prostate cancer (Beheshti *et al.*, 2010b; Beheshti *et al.*, 2010a) and another PET radiopharmaceutical such as ^{18}F-fluoromisonidazole (MISO) retains in hypoxic tissue and the tissue-to-blood ratio reveals the presence of hypoxic cells in head & neck tumours, brain tumours and breast tumours amongst others (Eschmann *et al.*, 2005; Wang *et al.*, 2010; Szeto *et al.*, 2009).

The wide range of possibilities that PET/CT presents in diagnostics and oncology makes the search for new diagnostic PET substances, new methods for quantifying activity and estimating tumour volumes in oncology a constantly increasing research area. If focusing on radiotherapy treatment planning; correct volume estimation is of utmost importance.

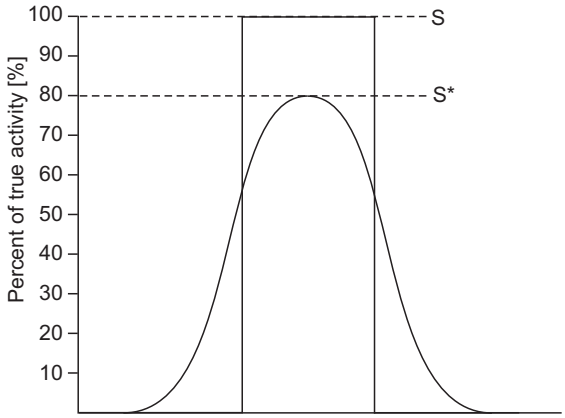

Figure 1. Illustration of the "spill-out" of signal caused by the PVE. S is the signal intensity corresponding to the true activity in a structure. S* is the signal intensity corresponding to the activity in the imaged structure.

Basing volume estimation on the anatomical information from CT imaging only can lead to large inaccuracies, since the anatomically visible tumour region not necessarily corresponds to the metabolically active tumour volume. Bradley *et al.* (2004) showed that the target volume changed in 50% of the cases when PET/CT was used for volume estimation in radiation therapy, compared to cases using only CT.

Partial volume effect in PET/CT

Although the impact of scatter and attenuation is large in PET images, the correction methods present today gives favourable results. One major difficulty that is still recognized in quantification of tomographic images is the partial volume effect (PVE) (Soret *et al.*, 2007), which gives deviations in quantification of the same order of magnitude as the effect of attenuation. This effect originates from the relatively poor spatial resolution of the tomographic system and thus has a major impact on the visualization and quantification of radionuclide uptake. The resolution in PET is however also degraded by the fundamental effect of positrons traveling a few millimetres in tissue before annihilation.

The partial volume effect is more pronounced in imaging of small structures, i.e. structures smaller than two to three times the full width at half maximum (FWHM) of the point spread function of the scanner, which commonly is of the size of 5 – 7 mm. This poses significant problems with the reliability of the activity values when imaging small structures, even when these structures are present in a surrounding with no background activity, which of course is never the case in real patient measurements.

The effect was discussed by Hoffman *et al.* already in 1979 and was expressed by the so-called recovery coefficient (RC) which was defined as the ratio of the activity derived from an image to the true activity in a structure (Hoffman *et al.*, 1979). The value of the RC is highly dependent of the size of the imaged structure.

As previously stated, the magnitude of the PVE depends on the size of the structure and the system resolution. But size and spatial resolution is not the only parameters affecting the magnitude of the PVE, but also the magnitude of the activity uptake, the shape of the structure and the amount and distribution of activity in surrounding tissues. The PVE could make a tumour uptake look less intense and thus could pose a problem for instance when using PET images in radiotherapy treatment planning, leading to that the tumours would look less aggressive than they really are (Vesselle *et al.*, 2000).

The PVE appears when the signal from inside a structure with a diameter smaller than 3 times the FWHM of the scanner is 'smeared' out into the neighbouring voxels, resulting in a lower apparent activity (Figure 1). It is implied that if a large enough region of interest is drawn around the uptake, the magnitude of the true activity can be derived, since no counts "disappears" but is only displaced due to the PVE. This is only valid if no background activity is present (Soret *et al.*, 2007). The term 'intensity diffusion', proposed by Skretting (2009), might be a better denomination, explaining the nature of the effect.

A problem in determining the magnitude of the PVE is that in the presence of a radioactive background, the signal from the background activity is of course also smeared out into adjacent voxels. This is called spill-in and the spread of signal from the structure towards the background is called spill-out and they both originate from the fact that the contour of the voxels does not correlate with the contour of the imaged structure. This can result in the presence of activity from two different structures in the same voxel. Methods for correction of PVE in PET imaging have been developed by several groups (Rousset *et al.*, 1998; De Bernardi *et al.*, 2009; Hoetjes *et al.*, 2010). A phantom for the assessment of detectability and PVE in tomographic systems has also recently been developed (Söderberg *et al.*, 2011) but to date, no solution has been widely accepted for the assessment or correction of the PVE.

Table 1. The recovery (RC) and partial volume effect (PVE)-corrected RCs for five sphere sizes and two ROI sizes (Paper II).

Sphere volume [ml] (diameter [mm])	RC	PVE-corrected RC, large ROI	PVE-corrected RC, small ROI
0.5 (10)	0.31	0.74	0.96
1 (12.5)	0.61	0.83	1.07
5.5 (22)	0.73	0.81	1.02
10.5 (27)	0.78	0.79	1.01
20 (34)	0.81	0.84	1.04

In paper II, the impact of tumour size and ROI size on the quantification was studied for a Philips Gemini TF PET/CT scanner and a number of different sphere sizes. Recovery coefficients obtained from phantom measurements of hollow spheres filled with a ^{18}F-FDG solution were used for a simple PVE correction method, which offers good results in the quantification of tumour uptake in tumours down to the diameter of 1 cm. It is calculated from the regional values in a specific ROI, thus it cannot be applied to an entire image. This is a simple correction which has to be determined for each PET/CT scanner and measurement approach and for each tumour size, but nevertheless it is widely used owing its ease of use (Geworski *et al.*, 2000; Hickeson *et al.*, 2002). After acquiring the RCs, they can be applied directly to the activity concentration values as follows: if the RC of a tumour is 0.31, the activity concentration value should be multiplied with 1/0.31, i.e. 3.2. Table 1 shows values of RC corrected as described above, using the previously obtained RC values (for small ROIs).

ROI definition

When determining the activity content in a structure, a ROI is drawn around the uptake and the number of counts in this region is derived. ROIs can be defined in a number of ways, every approach with its advantages and drawbacks. For instance, ROIs can be drawn as an isocontour which delineates a region including pixels exceeding a preset level in percentage of the maximum pixel value. The mean value of the number of counts in these pixels is then used as the tumour uptake.

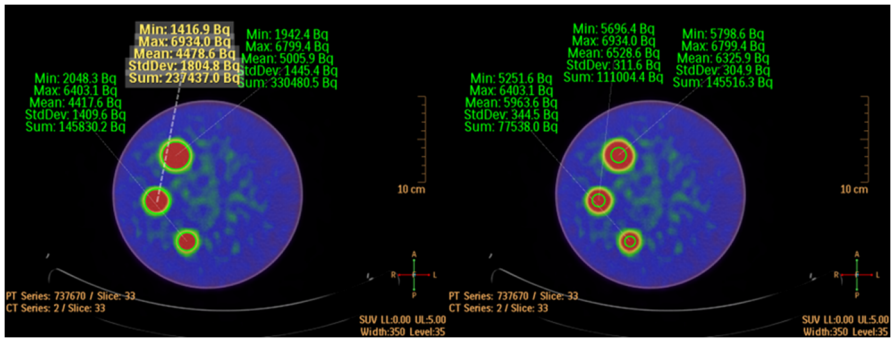

Figure 2. Left image show large ROI:s drawn at the boundary of the plastic walls of the spheres. Right image show small ROI:s drawn as to constitute approximately 40% of the large ROI:s. All ROI:s were drawn in the CT images and transferred into the PET images (Paper II).

Another approach is to use the maximum pixel alone as a measure of uptake. Both these approaches has the advantage of being user-independent, but the use of the maximum pixel value makes the method sensitive to noise. The PVE becomes smaller when the resolution becomes better, but a smaller pixel size would also result in more noise if the same number of counts were collected. The use of an isocontour ROI has the advantage of delineating the metabolically active part of a tumour and thus this approach could be in favour in staging of tumours. Manually drawing of ROIs is a very common approach, but the drawback of the user-dependence is obvious. On the other hand, an observer can look at both the CT and PET image and make a qualified assessment of the placement and size of the ROI and the risk of including activity from the background is smaller than in the use of isocontours, which could add the risk of background inclusion if the threshold is set too low. To make the method less user-dependent the size of the ROI could be fixed and thus independent of the size of the imaged structure. This approach could however make the assessment of inhomogeneous activity uptake difficult since only a small amount of voxels is included in the assessment. As in paper II, the ROIs can also be chosen to include a certain percentage of the anatomical boundaries derived from the CT image (40%) (Figure 2). This makes the influence of the PVE smaller, since the edges of the structure is not included in the activity quantification. If this is compared to the drawing of ROIs at the boundaries of the spheres in the CT image, the difference in fraction of the true activity from the image is on average 25% as seen in Figure 3 (Paper II).

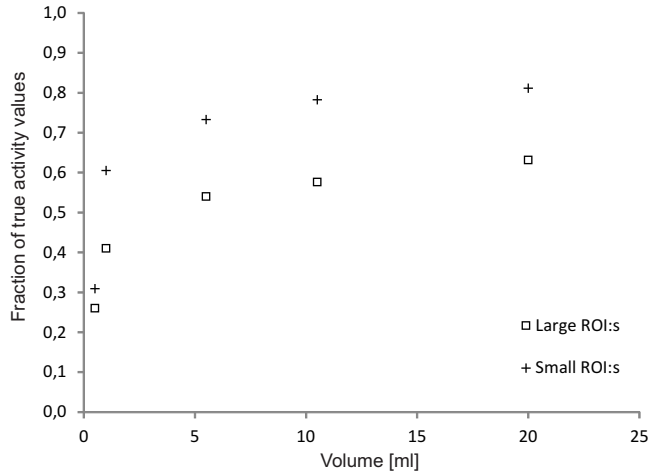

Figure 3. Fraction of true activity for large and small ROIs as a function of sphere size in the Jaszczak phantom. The lesion-to-background activity concentration ratio was 10:1. Large ROIs is the actual contour of the sphere, retrieved from the CT image. Small ROIs is 40 % of the actual contour of the sphere (Paper II).

Volume quantification

As previously mentioned, PET and foremost PET/CT has the potential of optimizing radiation therapy treatment planning by imaging of both anatomical regions as well as the metabolic behaviour of the tumour. In radiation therapy treatment planning, the ambition is to increase the irradiation of the target volume, and at the same time spare normal tissue from irradiation.

Accurate target delineation is a possibility of optimizing this further and both to keep the target volume as accurate as possible, but to make sure that no malignant tissue is excluded. The use of PET/CT as a tool in RT planning is steadily increasing due to the positive results presented in several studies (Bradley *et al.*, 2004; Beheshti *et al.*, 2010b; Higashi *et al.*, 2002).

Volume estimations can be based on the anatomical information from a CT image, but this can lead to large inaccuracies, since the anatomically visible tumour region and the metabolically active tumour volume does not necessarily correspond. Several different techniques for volume delineation have been developed and the need for a consensus regarding the choice of delineation method is essential. The difficulties with resolution and thus

the PVE must be assessed to be able to utilize the full potential of PET in delineation of target volumes.

Visual assessment of tumour volume is a very simple, subjective method, prone to user invariability. This approach implies that the nuclear medicine physicians are experienced and that they follow a carefully determined protocol to achieve accurate and reproducible results (Kiffer *et al.*, 1998). Automatic methods of volume delineation such as the use of an isocontour with a preset threshold value could result in the inclusion of background activity or activity in adjacent tissues if set too low. In the case of inhomogeneous activity uptake in a tumour, the isocontour could differ from the actual target volume needed for accurate RT. FDG is not tumour specific, and uptake of FDG also occurs within inflammatory tissue since the inflammatory processes also have an increased glucose metabolism.

Phantom measurements are essential in the evaluation of new delineation methods and the most common phantoms used in quantification in emission tomography are the Jaszczak phantom (Jaszczak *et al.*, 1984) and the NEMA NU-2 2001 phantom (Daube-Witherspoon *et al.*, 2002). Phantom experiments should reproduce the complexities of a clinical situation as closely as possible. However, commonly used phantoms typically consist of a circular or elliptical cylinder made of polymethyl methacrylate (PMMA) with fillable, hollow spheres for the simulation of tumour volumes. The presence of a non-radioactive wall between the hotspot and the background activity in these types of phantoms could lead to inaccuracies when interpreting the image data. The sphere wall has been shown to cause a decrease in the tumour-to-background (TBR) contrast and this could create inaccuracies in the volume estimation, especially for small tumours (Sossi *et al.*, 2001).

Phantom development

In paper III, a gelatin phantom without walls for use in quantification of activity and delineation of volume was developed. Eliminating the influence of phantom walls would make the phantom suitable for validation of activity and volume delineation methods. A few attempts have been made to develop phantoms without walls, but no attempts have so far become a regularly used method. This could be due to the complexity in the preparation process, which makes the preparation somewhat time-consuming and not so straight-forward for use in routine quality control (Bazanez-Borgert *et al.*, 2008; Turkington *et al.*, 2001).

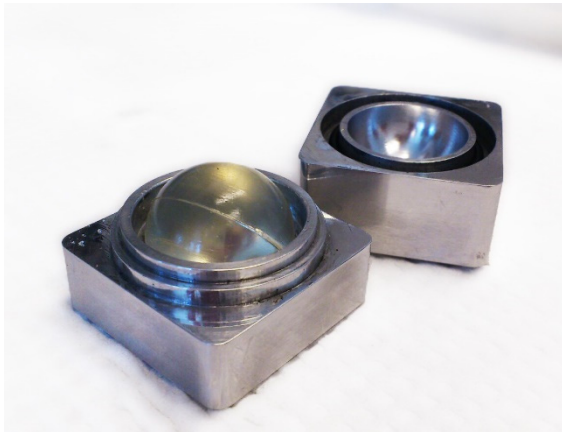

Figure 4. Aluminium mold with one of the ^{18}F-doped gelatin spheres (Paper III).

The preparation of radioactive spheres for the phantom measurements was made by using custom-made aluminium moulds of three different sizes. The largest aluminium mould and gelatin sphere is shown in Figure 4. A radioactive solution of dissolved gelatin and ^{18}F-FDG was poured into the moulds and then put in the freezer to solidify. The advantage with gelatin is that it is commercially available and that it is non-toxic. It easily dissolves in water, already at 40^{o}C and is solidified in 10 minutes for the smallest sphere and in 20 minutes for the largest sphere.

Three sizes of gelatin spheres were moulded, and for comparison three hollow, plastic spheres were filled with a solution with the same activity concentration. The inner diameter of the plastic, hollow spheres and the diameter of the gelatin spheres were: large spheres: 27.9 mm, medium spheres: 22.5 mm, small spheres: 15.6 mm. All spheres were placed in the outer cylinder of a Jaszczak phantom as shown in Figure 5 and imaged with a Philips Gemini TF PET/CT system.

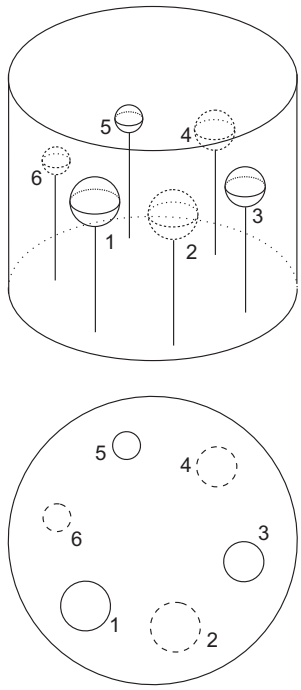

Figure 5. Illustration of the phantom including the placement of the hollow, plastic sphere inserts and the gelatin spheres. 1: Large plastic, 2: Large gelatin (ϕ: 27.9 mm), 3: Medium plastic, 4: Medium gelatin (ϕ: 22.5 mm), 5: Small plastic, 6: Small gelatin (ϕ: 15.6 mm) (Paper III).

Threshold-based volume delineation

A threshold-based volume delineation method, as described by van Dalen *et al.* (2007) and Hofheinz *et al.* (2010) was used for calculating the background corrected relative threshold level (T_{vol}) needed to correctly delineate the true sphere volume from emission images. In the studies of van Dalen *et al.* (2007) and Hofheinz *et al.* (2010), the influence of the inactive wall was theoretically determined. In paper III, this was done experimentally.

The method is based on the assumption that the activity in a point source in emission imaging can be described by a symmetric, three-dimensional (3D) Gaussian point spread function (PSF) (Hoetjes *et al.*, 2010). To simulate the spatial resolution blur in the image, an ideal sphere is convolved with the PSF. This approach is based on the method developed by Hofheinz *et al.* (2010), which in turn is based on the method developed by Kessler *et al.* (1984).

After the convolution, the radial activity profile across a sphere with a uniform activity distribution with no background activity present is described as:

$$P_z(z) = \begin{cases} \mathrm{erf}(Z) - \frac{2}{\sqrt{\pi}} Z e^{-Z^2} & (if\ z = 0) \\ \frac{1}{2}\mathrm{erf}(z+Z) - \mathrm{erf}(z-Z) - \frac{1}{2\sqrt{\pi}}\left[\frac{e^{-(z-Z)^2} - e^{-(z+Z)^2}}{z}\right] & (if\ z > 0) \end{cases} \quad \text{Eq. 4}$$

Z is the normalized sphere size with radius R, defined as:

$$Z = \frac{R}{\sigma\sqrt{2}} = \frac{2\sqrt{ln2}}{FWHM} R \quad \text{Eq. 5}$$

z is the radial coordinate corresponding to the radial position r, defined as:

$$z = \frac{r}{\sigma\sqrt{2}} \quad \text{Eq. 6}$$

and erf (Z) is the Gaussian error function, defined as:

$$\mathrm{erf}(Z) = \frac{2}{\sqrt{\pi}} \int_0^Z e^{-x^2}\, dx \quad \text{Eq. 7}$$

To make the equation valid for a sphere with true activity concentration S placed in a homogeneous background activity B, $P_z(z)$ is multiplied by the signal intensity minus the constant background, i.e.,$(S - B)$ and then the constant background B is added (Figure 6). The value of the radial activity concentration profile at each coordinate z is then given by:

$$A_z(z) = (S - B)P_z(z) + B. \quad \text{Eq. 8}$$

Correspondingly, the profile value at the sphere boundary is given by $A_z(Z)$ and this is thus the absolute threshold for correctly delineating the true sphere volume. $A_z(0)$ provides the signal amplitude in the centre of the sphere.

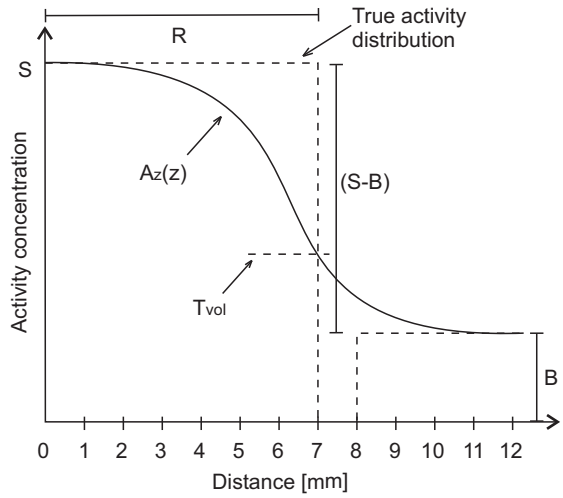

Figure 6. Illustration of the radial activity distribution in a sphere with a radius of 7 mm and a wall thickness of 1 mm. S is the signal intensity, B is the background intensity, $A_z(z)$is the radial activity concentration profile of a sphere with signal S surrounded by a background B, and T_{vol} is the background-corrected relative threshold (in percent of (S-B)) (Paper III).

For a sphere surrounded by a non-active wall w, the corresponding activity concentration profile is given by:

$$A_{z,w}(z) = S \cdot P_z(z) - B \cdot P_{z+w}(z) + B. \qquad \text{Eq. 9}$$

The background-corrected relative threshold T_{vol} is then defined as the ratio of the background-corrected absolute threshold to the background-corrected signal at the centre of the sphere (Eq. 10). For spheres with non-active walls the threshold is defined in a similar way using Eq. 9 instead of Eq. 8.

$$T_{vol} = \frac{A_z(Z)-B}{A_z(0)-B} \qquad \text{Eq. 10}$$

To calculate the threshold level based on imaging data from the PET measurements, the radial position of each voxel was associated with a radial coordinate and each value r, i.e. the distance from the centre of the sphere was used as input in MATLAB® and included in 10 000 numerical iterations to solve equation 10 and fit an isotropic Gaussian PSF to the experimental data.

Influence of phantom walls

The sphere wall has been seen to influence the value of the threshold needed for accurate delineation of sphere volume, This was theoretically determined by Hofheinz *et al.* (2010). The same influence can be seen in the experimental results of paper III, where it is verified that the threshold, T_{vol}, is decreased due to the sphere wall (Figure 7). This could result in an overestimation of the delineated volume of a tumour and thus the inclusion of a larger portion of normal tissues adjacent to the tumour if used in e.g. RT planning.

Another effect that is seen in phantom measurements is a dependence of the background fraction (BF), i.e. the threshold value drops with increasing background fraction. The background fraction is the reciprocal of the tumour-to-background ratio. This effect is well known and has been observed in several studies and is considered a significant problem in assessment of tumour volumes (Drever *et al.*, 2006; Cheebsumon *et al.*, 2011; van Dalen *et al.*, 2007). The background dependence is seen when conducting measurements using regular phantoms with plastic, hollow sphere inserts, but theoretically it has been determined to be an artefact of the measurements procedure due to the presence of sphere walls. Measurements of wall-less gelatin spheres, according to paper III validated the theoretically determined results (Figure 8). It is seen that the different background fractions indeed do not significantly influence the determination of T_{vol}. As a consequence, the threshold values estimated in phantom measurements using spheres with non-active walls should not be used for tumour delineation in patients as this would lead to erroneous volume estimations.

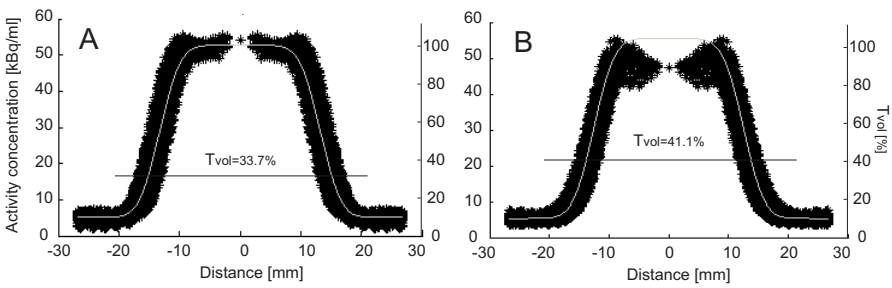

Figure 7. Measured radial activity concentration profile of the large gelatin sphere (left) and the large plastic sphere (right). An isotropic Gaussian PSF was fitted to the experimental data. The grey dotted line represents the background-corrected relative threshold, T_{vol} [%], which is the threshold value needed to correctly delineate the true sphere volume (Paper III).

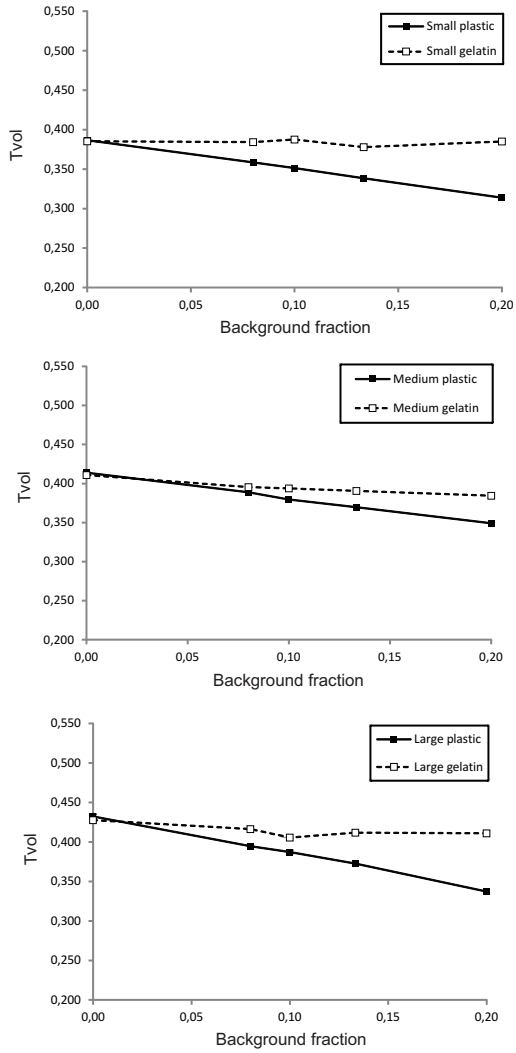

Figure 8. T_{vol} calculated in spheres of three sizes (ϕ: 27.9 mm, 22.5 mm, and 15.6 mm) as a function of background fraction (BF) with and without non-active walls (Paper III).

Biokinetic studies

Biokinetic studies aims at estimating the uptake, distribution and excretion of a radiopharmaceutical in the body over time. This kind of studies is conducted as a means of estimating the potential use of new radiopharmaceuticals and also in the evaluation of the radiation risks in proportion to their benefits. Knowledge of the uptake and excretion pattern of the radiopharmaceutical is essential in determining the radiation dose to organs and tissues after a diagnostic or therapeutic procedure in nuclear medicine.

The introduction of new imaging techniques as well as non-imaging techniques in nuclear medicine calls for new methods in determining the biokinetic behaviour of radiopharmaceuticals. Commonly, biokinetic studies are conducted on the basis of a series of planar gamma camera images. Planar images however, have the drawback of projecting three-dimensional distributions into two-dimensional images. This leads to difficulties in separating activity content in different organs and tissues. Activity quantification using planar gamma camera images also requires methods that correct for attenuation, scatter, activity in over- and underlying tissue and organ and body thickness. In estimating the organ and body thickness, two orthogonal projections can be of help. Corrections also have to be made in tomographic images but with the introduction of hybrid SPECT/CT and PET/CT scanners, e.g. the attenuation correction has become much more accurate than using radionuclide sources for transmission imaging (Berker *et al.*, 2011; He *et al.*, 2009; Mattsson and Skretting, 2011). A CT scan is acquired and the Hounsfield units in the CT image are converted into a map of attenuation coefficients of the chosen radiopharmaceutical distributed in the patient (Bai *et al.*, 2003; Brown *et al.*, 2008). As mentioned earlier, scatter correction can be made by e.g. the TEW method, but the choice of collimator type also has to be considered when choosing scatter correction method. In imaging of ^{123}I, the use of a low-energy collimator in combination with the TEW scatter correction method provides better results than the use of a medium-energy collimator (Rault *et al.*, 2007). Methods for SPECT image reconstruction include the use of filtered backprojection or iterative reconstruction methods. When using iterative reconstruction methods, the number of equivalent iterations (EI), i.e. the number of iterations and subsets can also affect the quantification. Reconstruction parameters must be chosen to

create the best conditions for each radiopharmaceutical and diagnosis (Söderberg *et al.*, 2012). In the diagnosis of neurodegenerative disorders, the number of EI shown to give good results for quantification of ^{123}I-FP-CIT images is between 80 and 100 (corresponding to 8 subsets and 10 iterations and 10 subsets and 10 iterations, respectively). The use of a higher number than 100 EI has been shown to increase the noise in the reconstructed image (Dickson *et al.*, 2010).

Dosimetric and biokinetic data of new radiopharmaceuticals for use in diagnostic and therapeutic nuclear medicine should be retrieved using the new imaging modalities present at nuclear medicine departments today. It would also be of interest to repeat biokinetic studies of radiopharmaceuticals already in use for the purpose of more accurate dose estimates. Another important aspect is to study the impact of age, gender and/or medication among patients and to perform biokinetic studies using subjects of different age groups and during medication for estimating differences in organ uptake due to these parameters. This should be done to make dose estimations reflecting the kinetics of the subjects of interest for each kind of diagnostic and therapeutic procedure.

Internal dosimetry

Since the radiation absorbed doses (or short; absorbed dose and even "dose") to organs and tissues cannot be measured, biokinetic and dosimetric models are needed to convert measurable quantities, such as data retrieved from planar or tomographic images and from measurements of administered and excreted activity to absorbed dose in tissues and organs. To estimate the absorbed dose and effective dose, the physical properties and the biological behaviour of the radiopharmaceutical has to be known. The absorbed dose is defined as the amount of energy from ionizing radiation that is absorbed per unit mass of the tissue and it has to be determined for each organ. It can then be used to calculate the mean absorbed dose to organs and tissues and the effective dose to a reference person (ICRP, 1975, 2002).

The mean absorbed dose for a specific organ according to the Committee on Medical Internal Radiation Dose (MIRD) of the Society of Nuclear Medicine and the International Commission on Radiological Protection (ICRP) is defined as:

$$D(r_T, T_D) = \sum_{r_s} \tilde{A}\,(r_s, T_D) S(r_T \leftarrow r_s) \qquad \text{Eq. 11}$$

where $\tilde{A}(r_s, T_D)$ is the cumulated activity defined as the total number of disintegrations in a particular source region, r_s, during a specific time interval, T_D and is thus calculated as the integral of the time-activity curve showing the retention of the radioactivity in the organ (Bolch *et al.*, 2009):

$$\tilde{A}(r_s, T_D) = \int_0^T A(r_s, t)\, dt \qquad \text{Eq. 12}$$

S is the so-called S-value which is defined as the mean absorbed dose in the target region per unit cumulated activity in the source region. The S-value is dependent on the mean energy emitted per disintegration, E_i, the number of nuclear transitions per nuclear transformation, Y_i, and the fraction of emitted energy from a source organ absorbed in the target organ per unit mass of the target organ, Φ_i. The S-value is thus expressed as:

$$S(r_T \leftarrow r_s) = \sum_i E_i Y_i \Phi_i\,(r_T \leftarrow r_s, E_i) \qquad \text{Eq. 13}$$

where r_s is the source organ and r_T is the target organ. The mean absorbed dose, D, is thus the relevant S–values multiplied by the cumulated activity which can be acquired experimentally by conducting a biokinetic study.

To estimate the effective dose, i.e. the whole body dose corresponding to the stochastic risks associated with all radiation-weighted organ doses, the following expression has been developed by the International Commission on Radiation Units and Measurements (ICRU) and the (ICRP):

$$E = \sum_T w_T \sum_R w_R D_R(r_T, T_D) \qquad \text{Eq. 14}$$

where w_R is the radiation weighting factor which takes the type of radiation into account (w_R =1 in the case of photons, electrons, positrons and β-particles) (ICRP, 2003) and w_T is the tissue weighting factor which takes the relative radiation sensitivity of the organs into account (ICRP, 2007).

The S-values for several individual pairs of source and target organs have been given by MIRD (Snyder *et al.*, 1975), based on the MIRD anthropomorphic phantom. This was the first mathematical phantom, describing the body and its organs by geometrical shapes. The RAdiation Dose Assessment Resource (RADAR) provides S-values for use in the OLINDA/EXM (Organ Level INternal Dose Assessment with EXponential Modelling) software (Stabin *et al.*, 2005; Stabin and Farmer, 2012) based

on the Cristy and Eckerman mathematical phantoms (Cristy and Eckerman, 1987) which are an extension of the MIRD phantom with phantoms describing a newborn, a 1-year-old, 5-, 10-, 15-year-old and the adult male and female. The mathematical phantoms give a simplified estimation of the human body and its organs and in order to make the estimations more realistic, phantoms with an improved anatomical description of the human body have been developed by Zankl and Petoussi-Henss (2002). These phantoms are so called voxel phantoms based on medical image data obtained from CT or MRI examinations on real persons. To be able to use the voxel phantoms for calculation of doses to reference persons according to the ICRP, the individual phantoms were adjusted to be representative of the adult Reference Male and Reference Female (ICRP, 2002). The ICRP voxel phantoms are referred to as ICRP-AM and ICRP-AF and is used by the ICRP to calculate dose coefficients for internal and external exposures (Smith *et al.*, 2001; Schlattl *et al.*, 2007; Li *et al.*, 2010). The voxel phantoms offer a better description of the human body and thus better estimations of the absorbed dose and effective dose but is not yet implemented in a commercially available dose calculation software.

Outline of a biokinetic study

The outline of a biokinetic study of a radiopharmaceutical is dependent on the effective half-time. The retention and excretion of the radiopharmaceutical is also of importance when choosing the time points for imaging or sampling. The time points have to be chosen so that both the uptake and the excretion phases are included, preferably with a shorter time interval in the uptake phase. It is often enough to choose a time span of the study of about four times the effective half-time (including the physical half-life and the biological half-time) of the radionuclide to study the biological behaviour.

During the time span of the study, PET/CT, SPECT/CT or gamma camera images are acquired at least at three time points after injection, but commonly five or more. More time points lead to better estimations of the time-activity curves for radiopharmaceuticals. Blood samples are collected, preferably in conjunction with imaging to determine the activity concentration in the blood at different time point p.i.. All urine are collected during the whole measurement period to determine the activity concentration in the urine. Faeces can also be gathered but this is not always applicable, e.g. if the biological half-time is very short or if patients are sent home during the measurement period and have a hard time collecting it themselves at home.

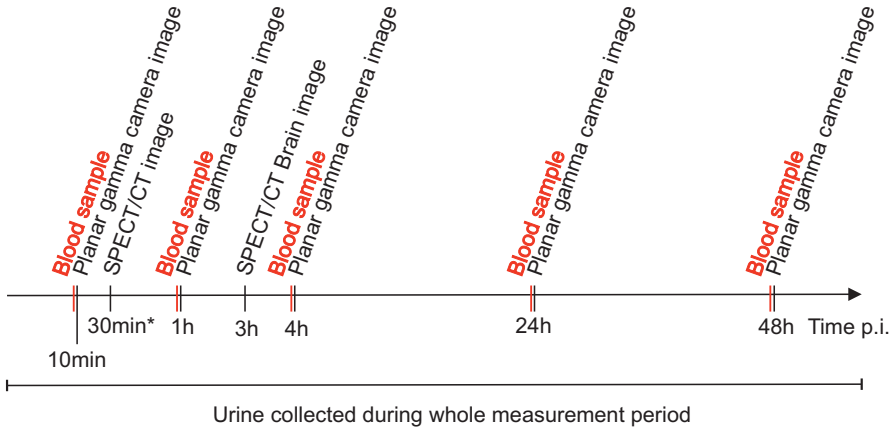

Figure 9. Outline of a biokinetic study of the biodistribution of ^{123}I-FP-CIT including planar gamma camera and SPET/CT scans as performed in Paper I. Blood samples were collected prior to each whole body scan. *The SPECT/CT thoracic/abdominal scan was acquired in conjunction with the first planar gamma camera scan, i.e. 20-30 min p.i..

Urine sampling can either be done by controlled sampling, i.e. the subjects are told to urinate at a certain time interval, or it can be done by collecting urine at the natural voiding interval of the subject. The imaging and sampling protocol for the investigation of the biodistribution of ^{123}I-FP-CIT, as performed in Paper I is shown in Figure 9.

^{123}I-FP-CIT is a cocaine analogue used in the staging and diagnosis of neurodegenerative disorders, e.g. Parkinson's disease, Alzheimer's disease and dementia with Lewy bodies (DLB) by serotonin imaging. The kinetics of FP-CIT is relatively fast and allow adequate striatal uptake for imaging 3 h post injection (p.i.) (Booij *et al.*, 1997). Ten patients with a mean age of 71 years were included in the study in Paper I for determination of the biodistribution and dosimetry of ^{123}I-FP-CIT in male patients of this age group. The distribution of ^{123}I-FP-CIT in a 65-year-old male patient with suspected Parkinsonism is shown at five time points in Figure 10 showing activity mainly concentrated in the liver, lungs and brain.

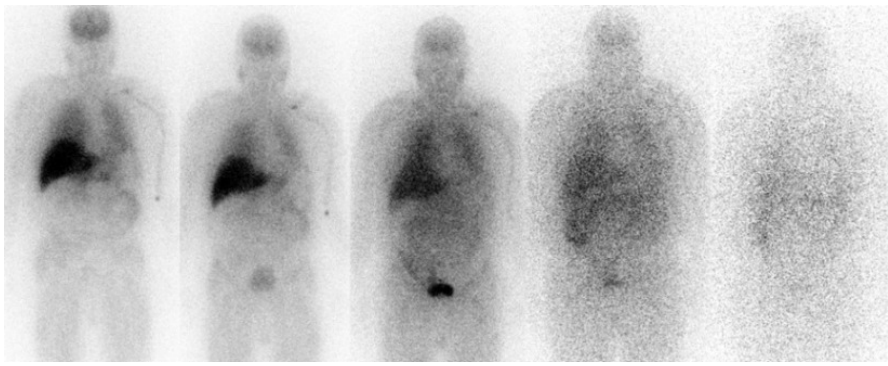

Figure 10. Anterior whole-body emission scans of a 65-year-old male patient with suspected Parkinsonism at five time points (10 min, 1 h, 4 h, 24 h and 48 h) after injection with 168 MBq of ^{123}I-FP-CIT (Paper I).

Figure 10 also visualizes the difficulties in quantification of planar gamma camera images mentioned earlier, and the fused SPECT/CT images from the same study (Paper I) show the advantages of tomographic imaging, such as better spatial resolution and separation of organs gained by tomographic imaging (Figure 11).

Biokinetic modelling

Clinical data, obtained from biokinetic studies in humans, can be analyzed simply by integrating the time-activity curves based on the experimentally obtained activity values. This method gives information on the total number of disintegrations in a source organ, but the transfer between source organs cannot be retrieved. A more complex method is the use of compartmental models describing the whole system, the deposition and retention of the radiopharmaceutical, the transfer between organs and tissues and the excretion pathways from the body (Giussani *et al.*, 2012). Modelling of biokinetic data can be made using a computer software, such as the Simulation Analysis And Modeling software (SAAMII) (Barrett *et al.*, 1998). A model consisting of a number of compartments representing e.g. blood, organs or excretion paths is created with the help of the program. SAAMII then creates systems of differential equations based on the structure of the model and the input of data (e.g. experimental) and simulates the solutions to these by an iterative fitting process. ICRP have a number of recommended biokinetic models for the alimentary tract, the respiratory tract, for the excretion pathways and for activity in the systemic circulation (ICRP, 2008b). The most common approach of modelling biokinetic data is to define the data as a series of exponential

terms (in this case the compartments). The equation used for estimating a time-activity curve for a specific compartment have the form:

$$A(t) = a_1 e^{-b_1 t} + a_2 e^{-b_2 t} + \ldots \quad \text{Eq. 15}$$

Assuming the coefficients a_i are fractions of administered activity and b_i are in the unit of time, the area under the time-activity curve is the normalized cumulated activity, $\tilde{A}/A_0$, defined as the number of disintegrations in a source region per unit administered activity.

If the transfer between compartments are considered, the description of the activity $A(i,t)$ in compartment i (as a part of a multicompartmental model) at time t, due to an intake at time t=0 can be described by:

$$A(i,t) = \prod_{k=1}^{i-1} \lambda(k,k+1) \sum_{k=1}^{i} \frac{A(1,0) e^{-(\lambda_k + \lambda_R)t}}{\prod_{p=1, p\neq k}(\lambda_p - \lambda_R)} \quad \text{Eq. 16}$$

where $\lambda(k,k+1)$ is the rate constant describing the transfer of material from compartment k to compartment k+1, A(1,0) is the activity in the first compartment at time t=0, λ_k is the rate constant for the total loss due to transfer from compartment k to other compartments and λ_R is the physical decay constant of the chosen radionuclide.

A multicompartmental model, based on the data obtained in Paper I, was created using the SAAM II© software (Barrett *et al.*, 1998) as shown in Figure 12. One central exchange compartment was included (blood), in which the activity was administered as a bolus injection. A series of sub-compartments were then connected to this compartment to represent the source organs that were clearly visible and imaged in all patients; liver, lungs, brain, spleen, small intestine (SI), upper large intestine (ULI), lower large intestine (LLI) and heart. A compartment that represented the rest of the body, termed the remainder compartment, was also added. Urine and faeces were considered to be excretion routes, and a urine voiding interval of 3.5 h was used, as recommended by the ICRP (1998). As faeces was not collected, the excretion via faeces was estimated from the model based on experimental data from the source organs and on urine excretion. Liver excretion into the gallbladder and gallbladder emptying was predicted using the liver and biliary excretion model, as suggested by ICRP 106 (ICRP, 2008a). The best fit to the experimental data for the liver, lungs, brain, spleen and heart was determined using the sum of two compartments: for liver, compartments 2 and 3; for lungs, compartments 4 and 5; for brain, compartments 10 and 11; for spleen, compartments 8 and 9; for heart, compartments 6 and 7.

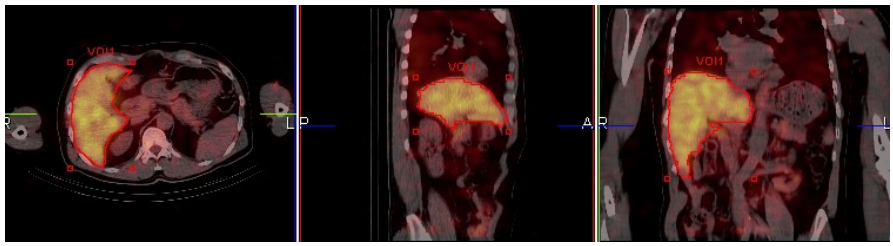

Figure 11. Fused SPECT/CT thoracic/abdominal images of an 80-year old patient, showing a representative organ volume-of-interest (VOI).

Time-activity curves were generated for all source regions as the compartmental model was fitted to the experimental data for each p.i. time point to calculate the number of disintegrations in all source regions per unit administered activity. Based on the number of disintegrations in the source regions, the absorbed organ doses could be calculated using the adult male model in the OLINDA/EXM1.1 code (Stabin *et al.*, 2005) based on the specific absorbed fractions and mathematical phantoms developed by Cristy and Eckerman (Cristy and Eckerman, 1987).

The comparison of the quantification and thus the dosimetry based on planar gamma camera images alone and the quantification and dosimetry including the use of complementary SPECT/CT measurements show that the absorbed dose to the liver differs significantly. The absorbed dose to the liver as estimated by the planar images alone was 0.045 ± 0.005 (mean ± standard error of the mean, SE) mGy/MBq compared to an estimated absorbed dose of 0.075 ± 0.008 mGy/MBq based on the combination of planar and SPECT/CT images. The absorbed dose estimations for the liver in this study thus differs by approximately 40 % depending on the methodology.

A study by Booij *et al.* (1998) included healthy volunteers at a mean age of 42 years, but the age of a typical patient referred for this kind of examination is mainly higher. Since the striatal FP-CIT binding have been seen to decrease significantly with age (Kuikka *et al.*, 1999; Lavalaye *et al.*, 2000), the quantification based on imaging of subjects of an age corresponding to the age of referred patients is a natural step in the optimisation of the dosimetry. Comparing the absorbed dose estimates from the study in Paper I (planar imaging) with the ones in the study by Booij *et al.* (1998) the dose estimates for the brain, heart and spleen, differ significantly as seen in Table 2.

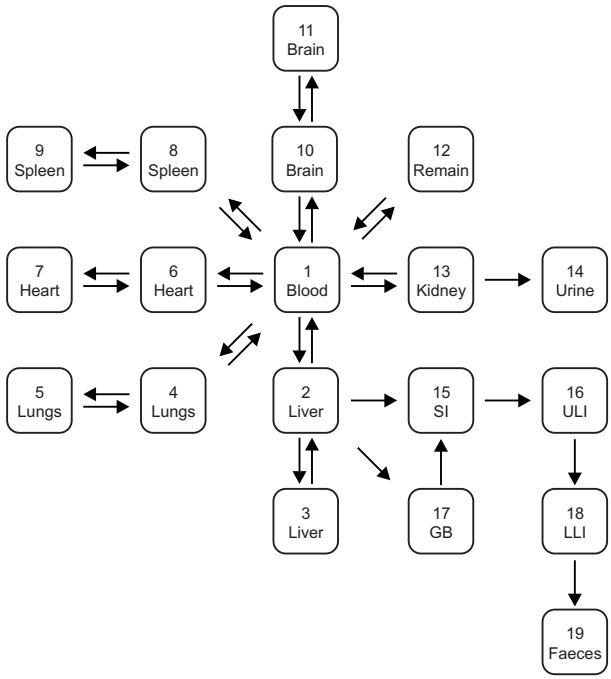

Figure 12. Diagram of the multicompartmental model used to generate time-activity curves for various organs in Paper I. GB, gall bladder; LLI, lower large intestine; Remain, remainder compartment; SI, small intestine; ULI, upper large intestine.

When estimating the number of disintegrations in the source regions per unit administered activity in the source organs and comparing the planar and planar combined with SPECT/CT methodology, substantial differences were seen in the values for the liver, spleen, SI, LLI and ULI (Table 3).

Table 2. Radiation absorbed dose estimates for ^{123}I-FP-CIT. Comparison between studies including subjects from different age groups. Mean age in Booij study is 42 yrs; mean age in Paper I study is 71 yrs. Values are given as mean ± standard deviation, SD.

Organ	Ave. dose; Boiij *et al.* [mGy/MBq]	Ave. dose; Paper I [mGy/MBq]
Brain	0.018 ± 0.005	0.011 ± 0.003
Heart	0.013 ± 0.001	0.028 ± 0.002
Spleen	0.011 ± 0.0009	0.022 ± 0.002

Table 3. The average number of disintegrations in source regions per unit of administered activity [h] (n = 10 patients).

Organ	Planar	Planar + SPECT/CT
Brain	0.476	0.532
Heart	0.240	0.255
Lower large intestine	0.474	0.371
Liver	2.025	4.026
Lungs	1.360	1.418
Small intestine	0.703	0.986
Spleen	0.206	0.127
Upper large intestine	0.760	0.372
Remainder	5.011	6.300

As shown in Table 3, the organ dose estimations differ significantly when different methods were used. These differences were mainly seen in organs that were not properly visualized in the planar images, such as the SI, ULI and LLI, and for organs with an irregular size and shape, such as the liver and the spleen. However, the effective dose is a robust quantity that is not affected substantially by the quantitative imaging methodology used for this type of measurement. Thus the use of complementary SPECT/CT measurements in biodistribution studies is merited in order to determine organ doses more accurately.

Microdosing

The development of new drugs is very expensive as well as time-consuming. The costs are steadily increasing as they are attributed to an increased failure rate of potential new drug candidates (DiMasi *et al.*, 2003; DiMasi *et al.*, 2010; Lappin and Garner, 2003). Estimates suggest that a pharmaceutical study – from molecule to approval for human use – takes on an average 10-15 years to perform. Add to that a failure rate of one in five candidates for which predictions made from animal testing do not correlate with the behaviour in humans and thus there is a pharmaceutical industry, and patients, in need of a more effective drug development regime. The requirements for a more time- and cost-effective drug development procedure including less preclinical animal experiments have promoted the development of methods for early screening in humans and have thus introduced the concept of microdosing. The human microdosing concept is aiming to speed up drug development and reducing the costs by improved candidate selection in early drug development (Garner and Lappin, 2006; Stenström *et al.*, 2010).

Microdosing was approved as a concept by the United States Food and Drug administration (FDA (2006)) and in a position paper from European Medicines Agency (EMEA (2004)) with the additional "note for guidance" from EMEA (2008). A microdose was then defined as: "less than $1/100^{th}$ of the pharmacological dose but a maximum of 100 µg."

Different analytical techniques such as AMS, PET, SPECT and LC-MS/MS can be used for analysis in microdose studies. AMS and PET is extremely sensitive and give information of the drug's pharmacokinetics, i.e. the absorption, distribution, metabolism and excretion (ADME). AMS and PET are relatively expensive techniques, but have the advantage of higher sensitivity (PET; 10^{-14} g, AMS; 10^{-18} g) than Liquid chromatography-tandem mass spectrometry (LC-MS/MS) (10^{-12} g) which is less expensive and have a greater availability (Bauer *et al.*, 2008). SPECT has a lower sensitivity than PET due to the collimation (parallel hole collimators). However, PET and SPECT complements each other in the imaging of different types of radionuclides such as; positron emitters for PET and single photon emitters for SPECT. The sensitivity is of great importance when administering as small amounts as in microdosing, thus the use of AMS and PET is increasing in clinical drug research. The use of SPECT is also increasing in drug development due to new collimation

techniques which increases the sensitivity of the system and also due to the abundance of SPECT systems and the wide range of radionuclides that can be used to label new molecules. One advantage in SPECT imaging is the physical half-lives of the photon emitters which are well suited for the examination times needed. The most frequently used SPECT radionuclides are ^{99m}Tc and ^{123}I which have physical half-lives of 6.02 h and 13.2 h respectively, in comparison with the PET substances ^{11}C and ^{18}F which have physical half-lives of 20.4 minutes and 110 minutes respectively. The drawback of the short half-lives of PET radionuclides is that a cyclotron is required in close vicinity to the research facility or clinic.

AMS and PET or SPECT can be used simultaneously for analysis of the behaviour of the same compound. The information acquired from the different modalities is complementary in that AMS, by blood and urine sampling, gives information about the pharmacokinetic profile in blood and urine and PET and SPECT gives information about the pharmacokinetic behaviour in different organs and tissues by imaging. An example of an important application of PET and SPECT microdosing is in the field of anticancer drug research (Van Dort *et al.*, 2008). In early drug development, an alternative to human data retrieved from microdosing with AMS, PET and SPECT is extrapolation of animal data. One advantage of the microdosing concept is thus implied; drug compounds for future human use should be tested in humans to decide upon whether it has the potential of reaching the market or not.

Microdose studies is also referred to as "Human Phase 0", implying that it is performed before the "Human Phase I" study which is the first time the drug is tested in man in a regular drug development study. The introduction of a "Phase 0" increases safety for human volunteers included in clinical studies since the amount of drug used is extremely small, thus the risk of a toxic reaction is considered minimal. A reduced safety package including a single-dose 14-day toxicology study in rat is conducted prior to a Phase 0 study (EMEA, 2008). This results in lower costs since the cost of a Phase I study is considerably higher than the cost of a microdose study including a reduced toxicology study (Wilding and Bell, 2005). The first in man testing is thus made earlier and minimizes the risk of rejection of new drugs after a long time of animal and toxicology testing leading to a decrease in the use of laboratory animals.

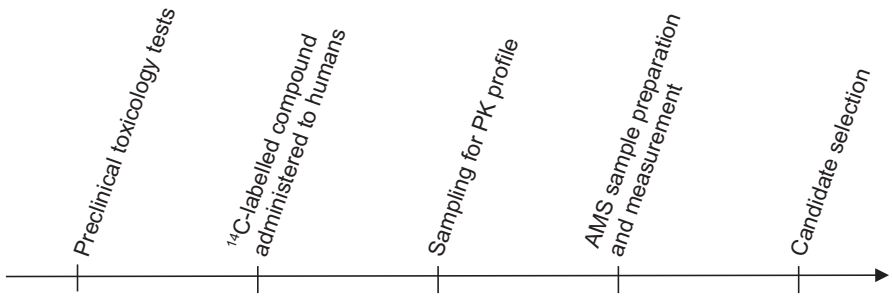

Figure 13. Outline of a microdosing study using accelerator mass spectrometry (AMS).

One issue with microdosing is whether the pharmacokinetics retrieved from a microdose can be extrapolated to the pharmacokinetics of a pharmacological amount. The question is if poor prediction of the PK of compounds at sub-pharmacological doses could lead to wrong decisions due to nonlinearities between a microdose and a pharmacological amount. A number of studies have evaluated the correlation between a microdose and a therapeutic amount e.g. the so-called Consortium for Resourcing and Evaluating AMS Microdosing (CREAM) trial (Lappin *et al.*, 2006) and the European Union Microdose AMS Partnership Programme (EUMAPP) project (Lappin *et al.*, 2011). The pharmacokinetic behaviour of a number of drugs were investigated and the candidate drugs were chosen as representing situations where pharmacokinetics might be difficult to predict using allometric scaling or physiologically-based models. The results of the CREAM trial looked promising but further evaluation of the microdosing concept was undertaken in the EUMAPP project (Lappin *et al.*, 2010; Lappin *et al.*, 2011). A recent review of the literature on microdosing studies reports that the pharmacokinetic data of a total of 35 compounds have been compared and 79 % of the orally administered compounds and 100 % of the intravenously administered compounds were scalable between a microdose and a therapeutic amount (Lappin *et al.*, 2013).

Microdosing with AMS is initiated with a toxicology study in rat and then the ^{14}C-labelling of the compound in question. After that, a microdose of the ^{14}C-labelled compound is orally or intravenously administered to a small group of human volunteers. Most commonly, blood and urine, and sometimes faeces are sampled at a number of time points post injection (p.i.) to determine the pharmacokinetic behaviour of the compound. Due to the extreme sensitivity of AMS, the amount of ^{14}C needed for analysis is very low and only results in an effective dose in the µSv range (Kim *et al.*, 2010). After sampling, the carbon in the samples has to be converted into elemental carbon by graphitization. Prior to graphitization, the samples can also be analysed by high-performance liquid chromatography (HPLC) to separate the metabolites of the drug (Lappin and Garner, 2003). The

conversion is done by combustion of samples, collecting the carbon dioxide formed in the process and reducing it over a carbon catalyst into graphite. The graphite is then pressed into aluminium cathodes which is placed in the AMS machine for analysis of the carbon content. The content of the radionuclide (^{14}C) reflects the amount of the pharmaceutical and its metabolites in urine and blood samples. Thus on the basis of data from the AMS analysis, the concentration of the parent drug and its metabolites in urine and blood can be calculated and the decision of whether the compound should proceed to Phase I or not can be taken (Figure 13).

Sample preparation

Production of high quality graphite targets is needed in the quantification of ^{14}C in biomedical samples. The graphitization process can be conducted in a number of ways depending whether high precision, short preparation time or easy handling is the most important for the specific situation (Vogel, 1992; Ognibene et al., 2003; Getachew et al., 2006; Xu et al., 2007; Sydoff and Stenström, 2010). In drug development, a fast and easily implemented sample preparation method is necessary, since the laborious sample preparation is one limiting factor in the implementation of the microdosing approach at the pharmaceutical companies. A compact, easy-to-handle AMS system is preferably combined with a simple and fast method of sample preparation to get the best throughput of samples as that would save both time and money.

The method developed in Paper IV is, compared to the conventional graphitization system developed by Stenstrom *et al.* (2010), a simplified, less laborious approach based on an original method by Vogel (1992) and the later methods by Ognibene *et al.* (2003) and Getachew *et al.* (2006). The method by Vogel (1992) included the use of torch-sealed quartz tubes for combustion of the samples and cryogenic removal of water from the samples before transfer of CO_2 to the reduction unit. The reduction units are also torch-sealed after the CO_2 transfer. Zink powder and hydrogen (in the form of TiH_2) were used in the reduction process and iron was used as a catalyst. Further development of the method was made by Ognibene *et al.* (2003) introducing septa-sealed vials for reduction instead of the torch-sealed quartz tubes and excluding the removal of water from the samples before transfer of CO_2. It was seen that the presence of water made the adding of TiH_2 redundant since the hydrogen gas formed when combusted water reacted with the zinc powder was sufficient for the catalytic reduction of CO_2.

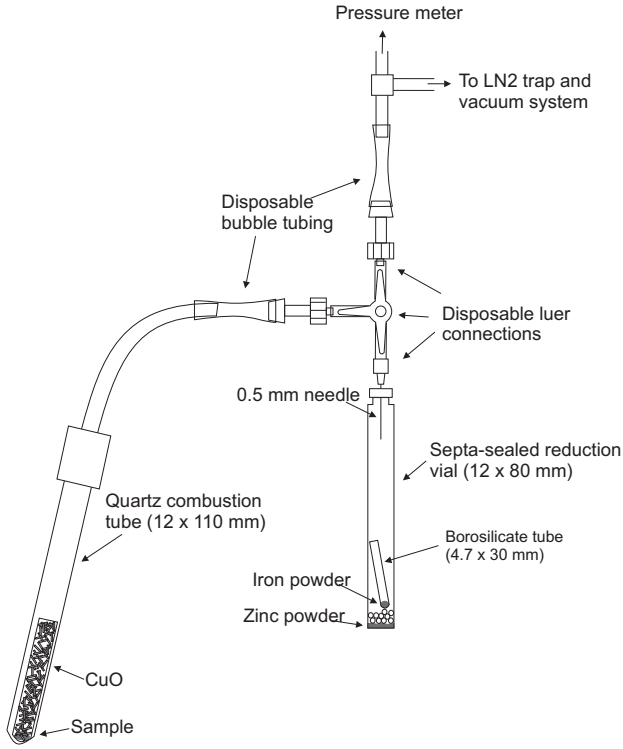

Figure 14. Schematic illustration of the simlified, online combustion system for graphitization of biomedical samples of septa-sealed vials (Paper IV).

The system developed in Paper IV is shown in Figure 14. The torch-sealed quartz tube used for combustion in the method by Ognibene *et al.* (2003) and Getachew *et al.* (2006) was replaced by a quartz tube connected online with the reduction unit with a luer-lock stopcock which was closed during combustion and opened during transfer of CO_2. The amounts of reagents used in the process were carefully controlled and tested for an optimal graphite yield. The amounts of zinc powder and iron catalyst were varied and it was seen that an increase of iron catalyst from 3-4 mg (Ognibene *et al.*, 2003) to 8 mg yielded higher $^{13}C^{+}$-currents and percent modern carbon (pMC) values very close to the reference values of the standards used in the measurements (sucrose standard; ANU, Oxalic acid standard; Ox I). The amount of added zinc powder was 120 mg, as that amount of zink was shown to maximize the $^{13}C^{+}$ current. The exclusion of TiH_2 from the reduction process, according to our measurements, increased the graphite yield by 50 % and $^{13}C^{+}$ currents by 25 %. After transfer of the CO_2 to the septa-sealed vial, the vial was immersed in liquid nitrogen to cryogenically trap the CO_2 before reduction. They were then heated to 550°C during 30 minutes and the temperature was maintained for 6.5 hours. The slow

heating was chosen to avoid a rapid start of the reduction process, which causes significant stress on the glass vials (Vogel *et al.*, 1984).

The chemical reactions that take place during the graphitization is:

$$CO_2 + Zn \leftrightarrow CO + ZnO$$

This reaction yields carbon monoxide which in turn reacts with the hydrogen gas formed in the reaction of the water from the sample and the zinc powder:

$$H_2O + Zn \leftrightarrow H_2 + ZnO$$

The carbon dioxide then reacts with the hydrogen gas to form water and carbon according to:

$$CO + H_2 \leftrightarrow C(s) + H_2O$$

The graphite/iron mixture was retrieved and pressed into aluminium cathodes which were placed in the AMS sample wheel for analysis. The measured pMC values for the measured standards were all within 2-3 % of the reference value of 150.61 pMC (ANU) and the reference value of 104.62 pMC (Ox I) (Paper IV). This is a precision that is sufficient for biomedical samples in microdosing studies (Figure 15).

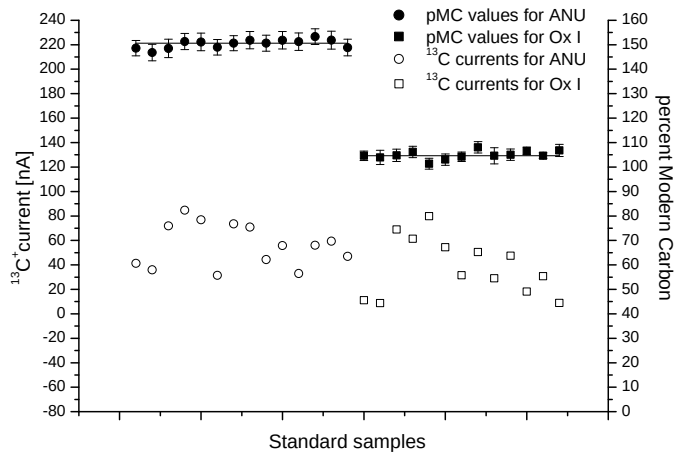

Figure 15. Average $^{13}C^{+}$ current and percent Modern Carbon (pMC) for ANU and Ox I standards prepared with the simplified graphitization system. Solid lines show reference values for ANU and Ox I (150.61 pMC and 104.62 pMC). Average values for measured samples are 150.38 pMC and 104.91 pMC respectively (Paper IV).

AMS analysis

The use of AMS as an extremely sensitive analytical tool for quantifying the ^{14}C content (i.e. counting of individual ^{14}C atoms) in biological samples is a two-step process. In the first step the carbon content in the sample is converted to graphite via the graphitization process as described in Paper IV and in the previous section. The second step is to analyse the carbon content to obtain the ratio of the radioactive isotope ^{14}C and the stable isotopes of carbon; ^{12}C and ^{13}C. The long half-life of ^{14}C of 5730 years makes decay counting methods, such as liquid scintillation counting impracticable and thus the capability in AMS to count individual atoms is favourable in the quantification of ^{14}C content in biomedical samples. AMS separates the different atoms based upon their mass, charge and energy difference and thus the ^{12}C, ^{13}C and ^{14}C content can be quantified simultaneously (Getachew *et al.*, 2006).

In order to facilitate implementation of the AMS technique closer to the clinics were the pharmacokinetic studies take place the development of smaller, cheaper and more easily operated AMS systems is a constantly ongoing process (Schulze-Konig *et al.*, 2010; Synal *et al.*, 2007; Wacker *et al.*, 2010). It is also a contributory cause to the development of applications for AMS analysis in several research disciplines.

The prepared graphite samples are placed in the sample wheel in the accelerator together with standard samples containing a known amount of ^{14}C and blanks which have no ^{14}C content. The accelerator used in Paper IV and Paper V is a single stage accelerator mass spectrometer (SSAMS) which is a relatively compact system, only occupying an area of approximately 6.5 x 5 m (Skog, 2007; Skog *et al.*, 2010). The SSAMS is a low voltage system i.e. operating at a maximum voltage of 250 kV, compared to the much larger, high voltage systems operating at voltages of 3 - 5 MV or higher (Garner *et al.*, 2000). The sample wheel is introduced into a caesium ion source in which the samples are bombarded with caesium vapour to form singly charged negative ions. The negative ion beam emerging from the sample consist mainly of $^{12}C^-$ (99 %) and $^{13}C^-$ (1 %) but also of $^{14}C^-$ (10^{-8} – 10^{-12} %) and molecular isobars of $^{14}C^-$, such as $^{13}CH^-$ and $^{12}CH_2^-$. The ion beam enters an injection magnet which is used for separating the ions based on their masses, which thus also permits the molecular isobars of ^{14}C into the mass 14 ion beam. The ion beams of mass 12, 13 and 14 are accelerated to a maximum of 250 keV and passed through a thin argon gas to dissociate the molecules and strip the valence electrons, leaving the ions in an average charge state of -1. After magnetically and electrically removing the positively charged fragments from the mass 14 beam, ^{14}C is measured using a particle detector at the end of the beamline. The $^{12}C^+$ and $^{13}C^+$ ion beams are deflected by a magnetic field towards two separately placed Faraday cups. The specific

activity of ^{14}C in the sample can then be determined after correction of background using the blanks and after comparison with the standard samples. The results from the AMS analysis are expressed as percent modern carbon (pMC); "modern carbon" referring to the ratio of $^{14}C/^{12}C$ in 1950, or $98 \cdot 10^{-18}$ mol ^{14}C/g carbon.

High vs. low voltage AMS

In Paper V, a comparison between a high voltage (5 MV) and a low voltage (250 kV) AMS system was made, analysing samples from the microdosing study EUMAPP including 152 selected samples consisting of 42 urine samples (6 samples of each of the 7 drugs fexofenadine, paracetamol, phenobarbital, sumatriptan, propafenone, Claritromycine and S-19812), 55 plasma samples (11 samples of each of 5 of the drugs fexofenadine, paracetamol, phenobarbital, sumatriptan and propafenone) and 55 HPLC fractions (11 samples of each of the 5 drugs: fexofenadine, paracetamol, phenobarbital, sumatriptan and propafenone). So called "graphites" were a group of samples graphitized with the graphitization system developed by Vogel (1992) and measured with both high voltage and low voltage AMS to make it possible to compare the AMS systems directly. In the analysis of the other samples, an inclusion of the different graphitization systems was made; the system used at the high voltage lab and the system described in Paper IV; allowing a comparison of the whole chain of graphitization and AMS system at the different sites. The high voltage system was placed at Xceleron, York, and the low voltage system was placed at Lund University.

The graphites were divided into three groups based on their approximate pMC values. High graphites were ~4500 pMC, medium graphites were ~1500 pMC and low graphites were ~350 pMC. The results of the direct comparison show that the systems were comparable, but the scatter of the data acquired at the high voltage system was larger than the data from the low voltage system (Figure 16). As seen in Table 4 the precision in the low voltage data is higher and the scatter (1 σ) of data is between 1.4 % and 2.2 %. Corresponding values for the high voltage data is between 3.9 % and 12.4 %.

The difference seen in the comparison between the high voltage and the low voltage machines could be due to different routines in operating the accelerators. Since routine with the low voltage AMS was that the sample wheel makes seven complete turns and routine with the high voltage AMS is that the sample wheel makes one single turn, this could be a reason for the differences in precision between measurements.

Table 4. Average and standard deviation values for low, medium and high graphites measured with low energy (LV) and high energy (HV) AMS systems (Paper V).

	High		**Medium**		**Low**	
	HV_{pMC}	LV_{pMC}	HV_{pMC}	LV_{pMC}	HV_{pMC}	LV_{pMC}
Mean	4527	4344	1571	1555	357.6	335.4
SD (1 σ)	176	94	107	23	44.4	4.7
% SD	3.89	2.17	6.82	1.50	12.42	1.39
% difference	4.04		1.02		6.21	

For the urine samples, plasma samples and HPLC fractions, different graphitization methods were used in conjunction with the low voltage and the high voltage AMS measurements. This was done to estimate the possible differences of the systems as used in routine measurements. This comparison make an assessment of the differences in results due to the choice of measurement procedure. If a pharmaceutical company would consider providing themselves with an AMS system (as well as a sample preparation lab), they would want to know the performance of such a system compared to the commercially available solutions such as engaging a company specialized at AMS analysis.

The analysis of the biological samples differed to a higher extent than the graphites. This is implied to be due to the differences in the graphitization procedure, but also due to handling of the samples which applies especially to the urine samples which showed the largest differences between measurements with the different systems (Figure 17). One reason that was suspected and later confirmed was loss of ^{14}C during vacuum centrifugation which was made prior to graphitization. Duplicates of some of the samples showing low pMC values, showed different results when using different centrifugation times. However, some of the urine samples were also measured with liquid scintillation counting (LSC) and the ratio between the low voltage measurements and the LSC measurements were much more consistent than the ratio between the low voltage measurements and the high voltage measurements. This could imply that the discrepancies between the LV AMS data and the HV AMS data is not due to differences between the accelerator systems but to differences in the condition of the sample material.

The corresponding results for the plasma samples and HPLC fractions is shown in Figure 18 and 19 respectively. Shown in figure 17, 18 and 19 is the ratio, R, between the low voltage and the high voltage data. The mean ratio of the plasma samples were 1.08 ± 0.32, 1.09 ± 0.25 for the HPLC fractions and 1.97 ± 2.39 for the urine samples.

This comparison show that low voltage and high voltage AMS machines are comparable with regard to precision although a slight difference was seen. This difference was however in favour of the low voltage machine, which is an indication of the good performance of such a system. When combining the AMS system with different graphitization procedures, larger differences were expected, but nevertheless the high-throughput system developed in Paper IV combined with the low voltage SSAMS system showed reasonable results with sufficient precision for measurement of biological samples from microdosing studies.

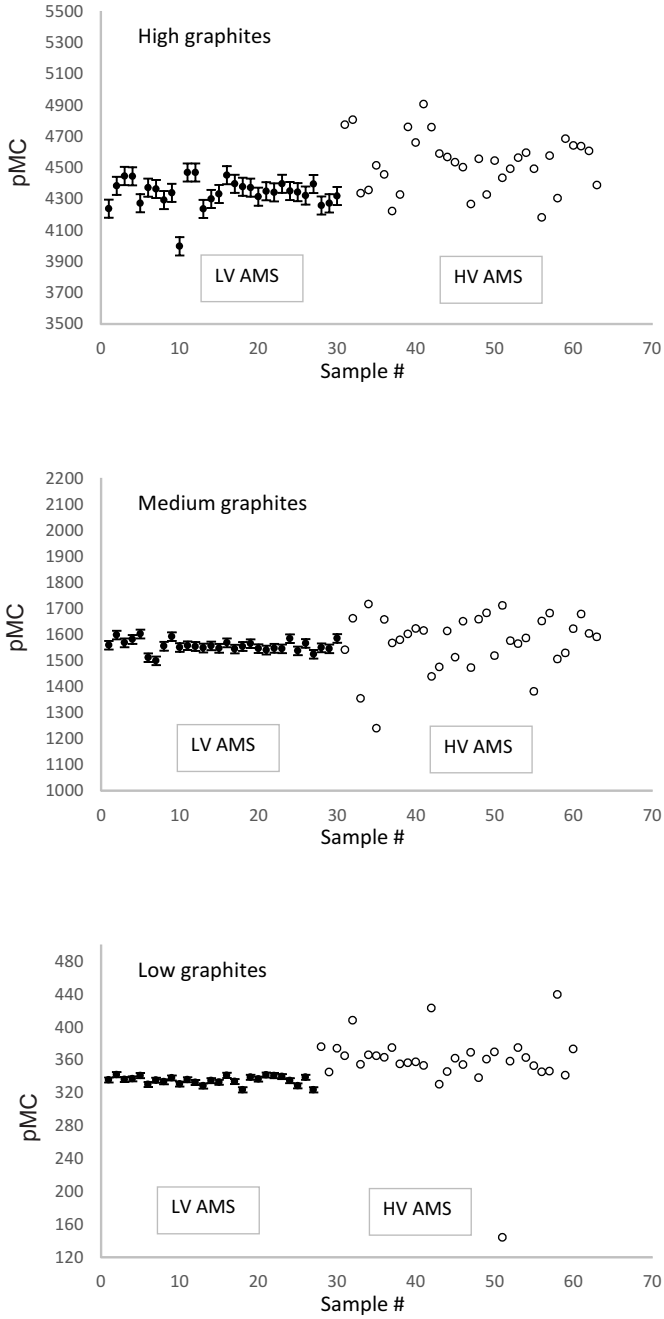

Figure 16. Comparison of high, medium and low graphites measured at the low voltage and the high voltage AMS system.

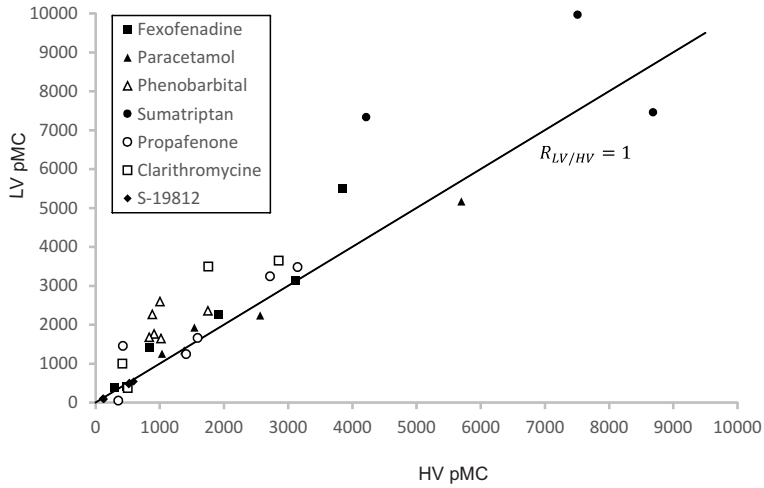

Figure 17. Comparison of pMC values for urine samples graphitized and measured separately at the high voltage (HV) and the low voltage (LV) AMS sites. The solid line represents the case of equal values (R=1).

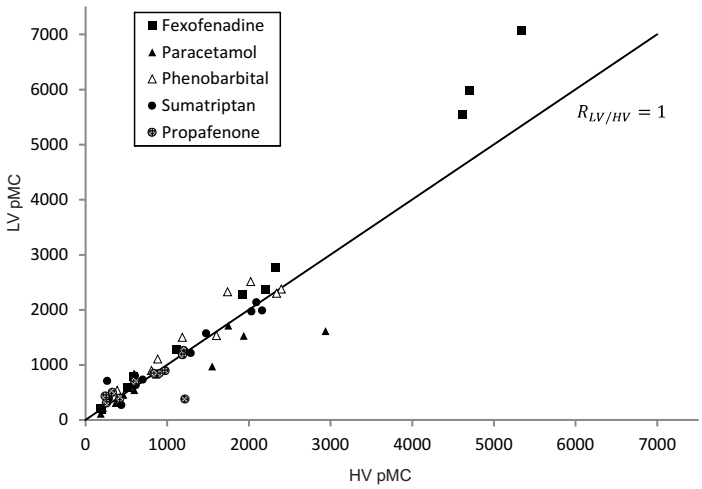

Figure 18. Comparison of pMC values for plasma samples graphitized and measured separately at the high voltage (HV) and the low voltage (LV) AMS sites. The solid line represents the case of equal values (R=1).

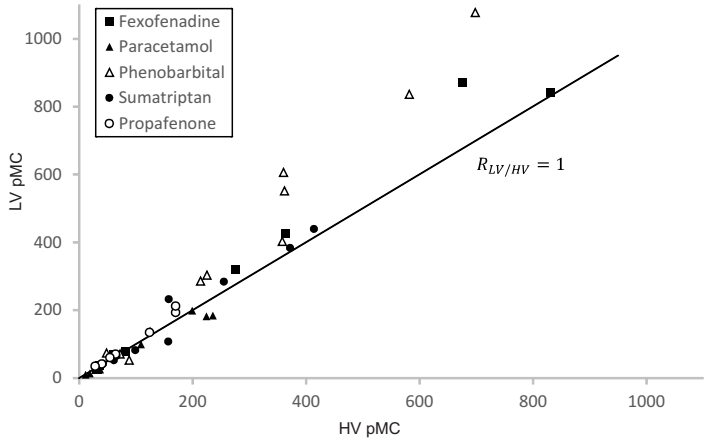

Figure 19. Comparison of pMC values for HPLC fractions graphitized and measured separately at the high voltage (HV) and the low voltage (LV) AMS sites. The solid line represents the case of equal values (R=1).

Conclusions

Determination of the biokinetic properties of a radiopharmaceutical is a complicated process, including corrections for system-specific parameters, patient measurements as well as modelling of patient data. It is a difficult task to model the behaviour of a compound in the human body, but as the methods are optimised, the approximations and the models becomes more and more accurate. The use of complementary SPECT/CT in the determination of the biodistribution and dosimetry, instead of using planar imaging alone is shown to be a better alternative in several ways. The absorbed doses to the organs are more accurately determined thus this should be done for other radiopharmaceuticals as well in order to recalculate the absorbed doses and effective dose. If the biokinetic behaviour is to be determined in patients and/or subjects of a high age, the duration of the measurement procedures are also of importance since they might have difficulties in lying in the camera for a long time. However, the approach of combining planar and tomographic imaging would overcome this and make use of the speed of the planar imaging and the accuracy of the SPECT/CT imaging.

In PET/CT imaging, the partial volume effect is a significant degrading factor due to the poor spatial resolution. The accuracy of activity and volume quantification is thus dependent on the development of correction methods which are able to correctly quantify the amount of the PVE. As of today, regions of interest are still often drawn manually and the method used influences the results of the quantification. Due to the large deviations from the true value when drawing regions manually, the use of more automated methods would be preferable. On the other hand, with the presence of hybrid scanners such as SPECT/CT and PET/CT, the observer can look at both the CT and the SPECT or PET image and make a qualified assessment of the placement and size of the ROI and thus the risk of including activity from the background would be smaller in this way.

The introduction of PET in radiotherapy treatment planning and monitoring of treatment response has increased the interest for development of methods for volume delineation. It is of great importance that the volume is correctly determined to give the best possible treatment to each patient. In assessment of volume and evaluation of volume delineation methods, phantom measurements are performed. The most

common phantoms place fillable, hollow spheres of different sizes in a circular or elliptical cylinder made of polymethyl methacrylate (PMMA). The spheres are filled with a radioactive solution and then imaged. The presence of plastic walls, however, leads to inaccuracies in quantification and should thus only be used when no background activity is present. The sphere walls causes a background dependence which is not present when imaging radioactive spheres without walls. The next step in use of the wall-less phantom would be to extend the measurements to study the accuracy of the threshold method for other shapes than spheres. The phantom could also be used to study the influence of movement on the detectability and volume estimation.

The concept of microdosing is of great interest in the pharmaceutical industry as it can shorten the time span for new drugs to reach the market and consequently save money. The use of AMS in microdosing is however a relatively expensive method which requires skilled personnel as well as a great deal of space as the AMS systems are comparatively large and somewhat complicated to run. But with an increasing interest from the pharmaceutical industry, the development towards smaller and more easily operated AMS systems is steadily increasing. The comparison between the larger high voltage systems and the smaller low voltage systems showed that the AMS instruments were comparable and that low voltage AMS provides a good alternative to high voltage AMS. To further promote the use of AMS for analysis of biomedical samples, the sample preparation method for preparing AMS targets also has to be fast and simple. The high-throughput graphitization system described in this thesis is such a method and it also showed reasonable results in measuring AMS standards and was suitable for measuring samples from microdosing studies. The combination of small-scale AMS and high-throughput graphitization thus provides a good alternative to the older more laborious graphitization systems and the more expensive high voltage AMS systems.

Acknowledgements

Den här boken hade aldrig blivit till om det inte hade varit för en massa andra personer som har hjälpt till på vägen. Hjälpt till på de sätt de kan, efter förmåga och ibland bara genom att finnas till.

Först och främst vill jag tacka mina handledare som hjälpt mig genom min doktorandtid och varit ett stöd på olika sätt (utan inbördes ordning):

Sigrid; tack för att du alltid är så glad och positiv! Du sporrar mig och gör mig alltid full av entusiasm inför nya utmaningar! Sören; Tack för att du trott på mig hela vägen och för att din dörr alltid står öppen när man behöver det! Kristina; du har varit ett stort stöd och en god vän. Tack för din aldrig sinande entusiasm och ditt stora kunnande – när jag blir stor vill jag bli som du! Helena; Tack för alla våra pratstunder om både jobb och annat! Det var ett nöje att ha dig som handledare – hoppas att vi kan jobba ihop igen någon dag!

Tack också till LEO för bra stöd och råd – jag vill dessutom poängtera att jag fick med MR i avhandlingen som utlovat ☺!

I also want to thank my eminent co-authors and international colleagues for their help with the manuscripts. Michael Stabin; for your help in making biokinetic modelling a little less incomprehensible. Augusto Giussani; for understanding the difficulties with patient studies and thus patiently waiting for our data. Graham Lappin; for your enthusiasm in our work long after the study was finished.

Tack till Eva, Ewa, Asal och Ing-Marie på KlinFys-avdelningen på SUS i Malmö för hjälpen med patienterna och ert tålamod med alla jobbiga extramätningar som jag ville ha gjorda! Tack också för ert glada humör och de trevliga pratstunder som man fick möjlighet att vara en del av.

Till mina nya kollegor i Helsingborg; tack för att ni fick mig att känna mig välkommen redan från första stund; ni är outstanding! Jag ser fram emot att få jobba med er i framtiden också!

Jag vill också tacka mina kära doktorandkollegor; utan er hade livet varit så mycket tråkigare! Flera av er räknar jag också som några av mina bästa vänner och det är något som jag värdesätter långt högre än doktorstiteln som jag också fick med mig på den här resan ☺. Tack; Pernilla för mycket trevligt rumssällskap med stickning, te och filt – och många djupa

diskussioner som inte alls hade med jobbet att göra; tack för ditt stöd (och för att du hittade den röda tråden som ingen annan gjorde)! Therése för alla våra mysiga fikapauser och diskussioner som också hade med allt annat än jobbet att göra - besvikelsen var stor de dagar du inte var på plats och gjorde livet gladare! Maria; för att du lyser upp med ditt glada humör jämt – fastän du har två småbarn hemma och knappt får sova något. Du är en kämpe – jag visste hela tiden att du skulle komma tillbaka ☺! Christian; för att du hängt kvar sedan studietiden och fortfarande verkar tycka att jag är en trevlig prick! Sofie; för att du är en solstråle som har lyst upp mina dagar många gånger! Martin; för trevligt sällskap under långa mätkvällar – tiden går så mycket snabbare när man har roligt! Fredrik; för alla matdiskussioner – så himla trevligt med någon som är lika matnördig som jag! Calle; för att du behärskar konsten att aldrig vika dig i en diskussion – oavsett om du har rätt eller inte ☺. Andreas; för trevligt sällskap som roomie – det blev inte så länge, men desto trevligare! Tack också till: Anna, Daniel, Marcus, Tony, Pontus, Unal, Mats, Magnus, Lars, Mattias, Simon, Jonas, Marie-Louise, Kalle och Peder för att ni gjort jobbet till en trevlig plats att åka till.

Tack Charlotta för trevliga diskussioner och stressterapi ☺; både på jobbet och fritiden - du vet hur mycket jag uppskattar det!

Tack även till mina vänner utanför jobbsfären som gör livet roligt att leva! Ni vet vem ni är och hur mycket ni betyder för mig!

Och sist men inte minst, tack till min familj;

Tack mamma och pappa för att ni format mig till den jag är idag.

Tack syrran för att du alltid har sagt att jag är bra – och menat det!

Tack Magnus för att du utmanar mig och gör mig till en bättre människa – du är underbar!

Tack Alexander för att du gör min värld till en bättre plats – du är fantastisk☺!

... utan er vore jag inget.

References

Anger H O 1958 Scintillation Camera *Review of Scientific Instruments* **29** 27-33

Anger H O, Price D C and Yost P E 1967 Transverse-Section Tomography with Scintillation Camera *Journal of Nuclear Medicine* **8** 314-&

Aston J A, Cunningham V J, Asselin M C, Hammers A, Evans A C and Gunn R N 2002 Positron emission tomography partial volume correction: estimation and algorithms *J Cereb Blood Flow Metab* **22** 1019-34

Bai C Y, Shao L, Da Silva A J and Zhao Z 2003 A generalized model for the conversion from CT numbers to linear attenuation coefficients *IEEE Trans Nucl Sci* **50** 1510-5

Barrett P H, Bell B M, Cobelli C, Golde H, Schumitzky A, Vicini P and Foster D M 1998 SAAM II: simulation, analysis, and modeling software for tracer and pharmacokinetic studies *Metabolism* **47** 484-92

Bauer M, Wagner C C and Langer O 2008 Microdosing studies in humans: the role of positron emission tomography *Drugs R D* **9** 73-81

Bazanez-Borgert M, Bundschuh R A, Herz M, Martinez M J, Schwaiger M and Ziegler S I 2008 Radioactive spheres without inactive wall for lesion simulation in PET *Z Med Phys* **18** 37-42

Beheshti M, Imamovic L, Broinger G, Vali R, Waldenberger P, Stoiber F, Nader M, Gruy B, Janetschek G and Langsteger W 2010a 18F choline PET/CT in the preoperative staging of prostate cancer in patients with intermediate or high risk of extracapsular disease: a prospective study of 130 patients *Radiology* **254** 925-33

Beheshti M, Vali R, Waldenberger P, Fitz F, Nader M, Hammer J, Loidl W, Pirich C, Fogelman I and Langsteger W 2010b The use of F-18 choline PET in the assessment of bone metastases in prostate cancer: correlation with morphological changes on CT *Mol Imaging Biol* **12** 98-107

Berker Y, Goedicke A, Kemerink G J, Aach T and Schweizer B 2011 Activity quantification combining conjugate-view planar scintigraphies and SPECT/CT data for patient-specific 3-D dosimetry in radionuclide therapy *Eur J Nucl Med Mol Imaging* **38** 2173-85

Bolch W E, Eckerman K F, Sgouros G and Thomas S R 2009 MIRD pamphlet No. 21: a generalized schema for radiopharmaceutical dosimetry--standardization of nomenclature *J Nucl Med* **50** 477-84

Booij J, Busemann Sokole E, Stabin M G, Janssen A G, de Bruin K and van Royen E A 1998 Human biodistribution and dosimetry of [123I]FP-CIT: a potent radioligand for imaging of dopamine transporters *Eur J Nucl Med* **25** 24-30

Booij J, de Jong J, de Bruin K, Knol R, de Win M M and van Eck-Smit B L 2007 Quantification of striatal dopamine transporters with 123I-FP-CIT SPECT is influenced by the selective serotonin reuptake inhibitor paroxetine: a double-blind, placebo-controlled, crossover study in healthy control subjects *J Nucl Med* **48** 359-66

Booij J, Speelman J D, Horstink M W and Wolters E C 2001 The clinical benefit of imaging striatal dopamine transporters with [123I]FP-CIT SPET in differentiating patients with presynaptic parkinsonism from those with other forms of parkinsonism *Eur J Nucl Med* **28** 266-72

Booij J, Tissingh G, Winogrodzka A, Boer G J, Stoof J C, Wolters E C and van Royen E A 1997 Practical benefit of [123I]FP-CIT SPET in the demonstration of the dopaminergic deficit in Parkinson's disease *Eur J Nucl Med* **24** 68-71

Bradley J, Thorstad W L, Mutic S, Miller T R, Dehdashti F, Siegel B A, Bosch W and Bertrand R J 2004 Impact of FDG-PET on radiation therapy volume delineation in non-small-cell lung cancer *Int J Radiat Oncol Biol Phys* **59** 78-86

Brown S, Bailey D L, Willowson K and Baldock C 2008 Investigation of the relationship between linear attenuation coefficients and CT Hounsfield units using radionuclides for SPECT *Appl Radiat Isotopes* **66** 1206-12

Buijs W C, Siegel J A, Boerman O C and Corstens F H 1998 Absolute organ activity estimated by five different methods of background correction *J Nucl Med* **39** 2167-72

Caldwell C B, Mah K, Ung Y C, Danjoux C E, Balogh J M, Ganguli S N and Ehrlich L E 2001 Observer variation in contouring gross tumor volume in patients with poorly defined non-small-cell lung tumors on CT: the impact of 18FDG-hybrid PET fusion *Int J Radiat Oncol Biol Phys* **51** 923-31

Cheebsumon P, Yaqub M, van Velden F H P, Hoekstra O S, Lammertsma A A and Boellaard R 2011 Impact of [F-18]FDG PET imaging parameters on automatic tumour delineation: need for improved tumour delineation methodology *Eur J Nucl Med Mol Imaging* **38** 2136-44

Cristy M and Eckerman K F 1987 Specific absorbed fractions of energy at various ages from internal photon sources. Volumes I-VII. Oak Ridge National Laboratory Report No: ORNL/TM-8381

Daisne J F, Duprez T, Weynand B, Lonneux M, Hamoir M, Reychler H and Gregoire V 2004 Tumor volume in pharyngolaryngeal squamous cell carcinoma: comparison at CT, MR imaging, and FDG PET and validation with surgical specimen *Radiology* **233** 93-100

Daube-Witherspoon M E, Karp J S, Casey M E, DiFilippo F P, Hines H, Muehllehner G, Simcic V, Stearns C W, Adam L E, Kohlmyer S and Sossi V 2002 PET performance measurements using the NEMA NU 2-2001 standard *Journal of Nuclear Medicine* **43** 1398-409

De Bernardi E, Faggiano E, Zito F, Gerundini P and Baselli G 2009 Lesion quantification in oncological positron emission tomography: a maximum likelihood partial volume correction strategy *Med Phys* **36** 3040-9

Derenzo S E, Zaklad H and Budinger T F 1975 Analytical study of a high-resolution positron ring detector system for transaxial reconstruction tomography *J Nucl Med* **16** 1166-73

Dewaraja Y, Li J and Koral K 1998 Quantitative I-131 SPECT with triple energy window compton scatter correction *IEEE Trans Nucl Sci* **45** 3109-14

Dickson J C, Tossici-Bolt L, Sera T, Erlandsson K, Varrone A, Tatsch K and Hutton B F 2010 The impact of reconstruction method on the quantification of DaTSCAN images *Eur J Nucl Med Mol Imaging* **37** 23-35

DiMasi J A, Feldman L, Seckler A and Wilson A 2010 Trends in risks associated with new drug development: success rates for investigational drugs *Clin Pharmacol Ther* **87** 272-7

DiMasi J A, Hansen R W and Grabowski H G 2003 The price of innovation: new estimates of drug development costs *Journal of health economics* **22** 151-85

Drever L, Robinson D M, McEwan A and Roa W 2006 A local contrast based approach to threshold segmentation for PET target volume delineation *Med Phys* **33** 1583-94

EMEA 2004 Position paper on non-clinical safety studies to support clinical trials with a single microdose. CPMP/SWP/2599.

EMEA 2008 Note for guidance on non-clinical safety pharmacology studies for human pharmaceuticals. CPMP/ICH/286/95.

Eschmann S M, Paulsen F, Reimold M, Dittmann H, Welz S, Reischl G, Machulla H J and Bares R 2005 Prognostic impact of hypoxia imaging with 18F-misonidazole PET in non-small cell lung cancer and head and neck cancer before radiotherapy *J Nucl Med* **46** 253-60

FDA 2006 US department of health and human services guidance for industry investigators and reviewers. Exploratory IND studies.

Fleming J S 1979 A technique for the absolute measurement of activity using a gamma camera and computer *Phys Med Biol* **24** 176-80

Garner R C, Barker J, Flavell C, Garner J V, Whattam M, Young G C, Cussans N, Jezequel S and Leong D 2000 A validation study comparing accelerator MS and liquid scintillation counting for analysis of 14C-labelled drugs in plasma, urine and faecal extracts *J Pharm Biomed Anal* **24** 197-209

Garner R C and Lappin G 2006 The phase 0 microdosing concept *Br J Clin Pharmacol* **61** 367-70

Gates G F 1983 Split renal function testing using Tc-99m DTPA. A rapid technique for determining differential glomerular filtration *Clin Nucl Med* **8** 400-7

Getachew G, Kim S H, Burri B J, Kelly P B, Haack K W, Ognibene T J, Buchholz B A, Vogel J S, Modrow J and Clifford A J 2006 How to convert biological carbon into graphite for AMS *Radiocarbon* **48** 325-36

Geworski L, Knoop B O, de Cabrejas M L, Knapp W H and Munz D L 2000 Recovery correction for quantitation in emission tomography: a feasibility study *Eur J Nucl Med* **27** 161-9

Giussani A, Janzen T, Uusijarvi-Lizana H, Tavola F, Zankl M, Sydoff M, Bjartell A, Leide-Svegborn S, Soderberg M, Mattsson S, Hoeschen C and Cantone M C 2012 A compartmental model for biokinetics and dosimetry of 18F-choline in prostate cancer patients *J Nucl Med* **53** 985-93

He B, Wahl R L, Sgouros G, Du Y, Jacene H, Kasecamp W R, Flinn I, Hammes R J, Bianco J, Kahl B and Frey E C 2009 Comparison of organ residence time estimation methods for radioimmunotherapy dosimetry and treatment planning--patient studies *Med Phys* **36** 1595-601

Hickeson M, Yun M, Matthies A, Zhuang H, Adam L E, Lacorte L and Alavi A 2002 Use of a corrected standardized uptake value based on the lesion size on CT permits accurate characterization of lung nodules on FDG-PET *Eur J Nucl Med Mol Imaging* **29** 1639-47

Higashi K, Ueda Y, Arisaka Y, Sakuma T, Nambu Y, Oguchi M, Seki H, Taki S, Tonami H and Yamamoto I 2002 F-18-FDG uptake as a biologic prognostic factor for recurrence in patients with surgically resected non-small cell lung cancer *Journal of Nuclear Medicine* **43** 39-45

Hoetjes N J, van Velden F H, Hoekstra O S, Hoekstra C J, Krak N C, Lammertsma A A and Boellaard R 2010 Partial volume correction strategies for quantitative FDG PET in oncology *Eur J Nucl Med Mol Imaging* **37** 1679-87

Hoffman E J, Huang S C and Phelps M E 1979 Quantitation in Positron Emission Computed-Tomography .1. Effect of Object Size *J Comput Assist Tomogr* **3** 299-308

Hofheinz F, Dittrich S, Potzsch C and Hoff J 2010 Effects of cold sphere walls in PET phantom measurements on the volume reproducing threshold *Phys Med Biol* **55** 1099-113

Hutton B F, Buvat I and Beekman F J 2011 Review and current status of SPECT scatter correction *Phys Med Biol* **56** R85-112

ICRP 1975 Report of the task group on reference man. ICRP Publication 23 *Ann. ICRP*

ICRP 1998 Radiation dose to patients from radiopharmaceuticals (addendum 2 to ICRP publication 53) ICRP publication 80 *Ann ICRP* **28** 1-126

ICRP 2002 Basic Anatomical and Physiological Data for Use in Radiological Protection Reference Values. ICRP Publication 89. *Ann. ICRP* **32**

ICRP 2003 Relative Biological Effectiveness, Radiation Weighting and Quality Factor". ICRP Publication 92. *Ann. ICRP* **33**

ICRP 2007 The 2007 Recommendations of the International Commission on Radiological Protection. ICRP publication 103 *Ann ICRP* **37** 1-332

ICRP 2008a Radiation dose to patients from radiopharmaceuticals. (Addendum 3 to ICRP Publication 53) ICRP Publication 106. *Ann ICRP* **38** 1-197

ICRP 2008b Radiation dose to patients from radiopharmaceuticals. Addendum 3 to ICRP Publication 53. ICRP Publication 106. Approved by the Commission in October 2007 *Ann ICRP* **38** 1-197

Jaszczak R J, Greer K L, Floyd C E, Harris C C and Coleman R E 1984 Improved Spect Quantification Using Compensation for Scattered Photons *Journal of Nuclear Medicine* **25** 893-900

Jaszczak R J, Murphy P H, Huard D and Burdine J A 1977 Radionuclide emission computed tomography of the head with 99mCc and a scintillation camera *J Nucl Med* **18** 373-80

Jönsson L, Ljungberg M and Strand S E 2005 Evaluation of accuracy in activity calculations for the conjugate view method from Monte Carlo simulated scintillation camera images using experimental data in an anthropomorphic phantom *J Nucl Med* **46** 1679-86

Keilson J and Waterhouse C 1978 Possible impact of the new spectrometric techniques on ^{14}C tracer kinetic studies in medicine. In: *First Conference on Radiocarbon Dating with Accelerators,* ed H E Gove (University of Rochester p 391

Kessler R M, Ellis J R, Jr. and Eden M 1984 Analysis of emission tomographic scan data: limitations imposed by resolution and background *J Comput Assist Tomogr* **8** 514-22

Keyes J W, Jr., Orlandea N, Heetderks W J, Leonard P F and Rogers W L 1977 The Humongotron--a scintillation-camera transaxial tomograph *J Nucl Med* **18** 381-7

Kiffer J D, Berlangieri S U, Scott A M, Quong G, Feigen M, Schumer W, Clarke C P, Knight S R and Daniel F J 1998 The contribution of 18F-fluoro-2-deoxy-glucose positron emission tomographic imaging to radiotherapy planning in lung cancer *Lung Cancer* **19** 167-77

Kim S H, Kelly P B and Clifford A J 2010 Calculating radiation exposures during use of (14)C-labeled nutrients, food components, and biopharmaceuticals to quantify metabolic behavior in humans *J Agric Food Chem* **58** 4632-7

King M A, Hademenos G J and Glick S J 1992 A dual-photopeak window method for scatter correction *J Nucl Med* **33** 605-12

Kojima A, Takaki Y, Matsumoto M, Tomiguchi S, Hara M, Shimomura O, Koga Y and Takahashi M 1993 A preliminary phantom study on a proposed model for quantification of renal planar scintigraphy *Med Phys* **20** 33-7

Krak N C, Hoekstra O S and Lammertsma A A 2004 Measuring response to chemotherapy in locally advanced breast cancer: methodological considerations *Eur J Nucl Med Mol Imaging* **31** Suppl 1 S103-11

Kuikka J T, Tupala E, Bergstrom K A, Hiltunen J and Tiihonen J 1999 Iodine-123 labelled PE2I for dopamine transporter imaging: influence of age in healthy subjects *Eur J Nucl Med* **26** 1486-8

Lappin G and Garner R C 2003 Big physics, small doses: the use of AMS and PET in human microdosing of development drugs *Nat Rev Drug Discov* **2** 233-40

Lappin G, Kuhnz W, Jochemsen R, Kneer J, Chaudhary A, Oosterhuis B, Drijfhout W J, Rowland M and Garner R C 2006 Use of microdosing to predict pharmacokinetics at the therapeutic dose: experience with 5 drugs *Clin Pharmacol Ther* **80** 203-15

Lappin G, Noveck R and Burt T 2013 Microdosing and drug development: past, present and future *Expert Opin Drug Metab Toxicol* **9** 817-34

Lappin G, Shishikura Y, Jochemsen R, Weaver R J, Gesson C, Houston B, Oosterhuis B, Bjerrum O J, Rowland M and Garner C 2010 Pharmacokinetics of fexofenadine: evaluation of a microdose and assessment of absolute oral bioavailability *Eur J Pharm Sci* **40** 125-31

Lappin G, Shishikura Y, Jochemsen R, Weaver R J, Gesson C, Houston J B, Oosterhuis B, Bjerrum O J, Grynkiewicz G, Alder J, Rowland M and Garner C 2011 Comparative pharmacokinetics between a microdose and therapeutic dose for clarithromycin, sumatriptan, propafenone, paracetamol (acetaminophen), and phenobarbital in human volunteers *European Journal of Pharmaceutical Sciences* **43** 141-50

Larsson A, Johansson L, Sundstrom T and Ahlstrom K R 2003 A method for attenuation and scatter correction of brain SPECT based on computed tomography images *Nucl Med Commun* **24** 411-20

Lavalaye J, Booij J, Reneman L, Habraken J B and van Royen E A 2000 Effect of age and gender on dopamine transporter imaging with [123I]FP-CIT SPET in healthy volunteers *Eur J Nucl Med* **27** 867-9

Leide-Svegborn S 1999 Radiation exposure of the patient in diagnostic nuclear medicine. In: *Department of Radiation Physics*: Lund University)

Li W B, Zankl M, Schlattl H, Petoussi-Henss N, Eckerman K F, Bolch W E, Oeh U and Hoeschen C 2010 Impact on 141Ce, 144Ce, 95Zr, and 90Sr beta emitter dose coefficients of photon and electron SAFs calculated with ICRP/ICRU reference adult voxel computational phantoms *Health Phys* **99** 503-10

Mattsson S and Skretting A 2011 ed M Cantone and C Hoeschen (Heidelberg: Springer)

Minarik D, Sjogreen K and Ljungberg M 2005 A new method to obtain transmission images for planar whole-body activity quantification *Cancer Biother Radiopharm* **20** 72-6

Mukai T, Links J M, Douglass K H and Wagner H N 1988 Scatter Correction in Spect Using Non-Uniform Attenuation Data *Phys Med Biol* **33** 1129-40

Norrgren K, Svegborn S L, Areberg J and Mattsson S 2003 Accuracy of the quantification of organ activity from planar gamma camera images *Cancer Biother Radiopharm* **18** 125-31

Ognibene T J, Bench G, Vogel J S, Peaslee G F and Murov S 2003 A high-throughput method for the conversion of CO2 obtained from biochemical samples to graphite in septa-sealed vials for quantification of 14C via accelerator mass spectrometry *Anal Chem* **75** 2192-6

Pandit N, Gonen M, Krug L and Larson S M 2003 Prognostic value of [18F]FDG-PET imaging in small cell lung cancer *Eur J Nucl Med Mol Imaging* **30** 78-84

Pereira J M, Stabin M G, Lima F R, Guimaraes M I and Forrester J W 2010 Image quantification for radiation dose calculations--limitations and uncertainties *Health Phys* **99** 688-701

Rault E, Vandenberghe S, Van Holen R, De Beenhouwer J, Staelens S and Lemahieu I 2007 Comparison of image quality of different iodine isotopes (I-123, I-124, and I-131) *Cancer Biother Radiopharm* **22** 423-30

Rousset O G, Ma Y and Evans A C 1998 Correction for partial volume effects in PET: principle and validation *J Nucl Med* **39** 904-11

Savolainen S 1992 SPECT versus planar scintigraphy for quantification of splenic sequestration of 111In-labelled platelets *Nucl Med Commun* **13** 757-63

Schlattl H, Zankl M and Petoussi-Henss N 2007 Organ dose conversion coefficients for voxel models of the reference male and female from idealized photon exposures *Phys Med Biol* **52** 2123-45

Schulze-Konig T, Dueker S R, Giacomo J, Suter M, Vogel J S and Synal H A 2010 BioMICADAS: Compact next generation AMS system for pharmaceutical science *Nucl Instrum Meth B* **268** 891-4

Sjögreen K, Ljungberg M and Strand S E 2002 An activity quantification method based on registration of CT and whole-body scintillation camera images, with application to 131I *J Nucl Med* **43** 972-82

Skog G 2007 The single stage AMS machine at Lund University: Status report *Nucl Instrum Meth B* **259** 1-6

Skog G, Rundgren M and Skold P 2010 Status of the Single Stage AMS machine at Lund University after 4 years of operation *Nucl Instrum Meth B* **268** 895-7

Skretting A 2009 'Intensity diffusion' is a better description than 'partial volume effect' *Eur J Nucl Med Mol Imaging* **36** 536-7

Smith T J, Phipps A W, Petoussi-Henss N and Zankl M 2001 Impact on internal doses of photon SAFs derived with the GSF adult male voxel phantom *Health Phys* **80** 477-85

Snyder W S, Ford M R, Warner G G and Watson S B 1975 "S", Absorbed Dose per Unit Cumulated Activity for Selected Radionuclides and Organs. *MIRD Pamphlet No. 11, The Society of Nuclear Medicine, New York.*

Soret M, Bacharach S L and Buvat I 2007 Partial-volume effect in PET tumor imaging *J Nucl Med* **48** 932-45

Sossi V, Pointon B, Boudoux C, Cohen P, Hudkins K, Jivan S, Nitzek K, deRosario J, Stevens C and Ruth T J 2001 NEMA NU 2-2000 performance measurements on an ADAC MCD camera *IEEE Trans Nucl Sci* **48** 1518-23

Stabin M and Farmer A 2012 OLINDA/EXM 2.0: The new generation dosimetry modeling code *J Nucl Med meeting abstracts.* **53** 585

Stabin M G, Sparks R B and Crowe E 2005 OLINDA/EXM: the second-generation personal computer software for internal dose assessment in nuclear medicine *J Nucl Med* **46** 1023-7

Stenstrom K, Unkel I, Nilsson C M, Raaf C and Mattsson S 2010 The use of hair as an indicator of occupational 14C contamination *Radiat Environ Biophys* **49** 97-107

Stenström K, Sydoff M and Mattsson S 2010 Microdosing for early biokinetic studies in humans *Radiat Prot Dosimetry* **139** 348-52

Sydoff M and Stenström K 2010 C-14 sample preparation for AMS microdosing studies at Lund University using online combustion and septa-sealed vials *Nucl Instrum Meth B* **268** 924-6

Synal H A, Stocker M and Suter M 2007 MICADAS: A new compact radiocarbon AMS system *Nucl Instrum Meth B* **259** 7-13

Szeto M D, Chakraborty G, Hadley J, Rockne R, Muzi M, Alvord E C, Jr., Krohn K A, Spence A M and Swanson K R 2009 Quantitative metrics of net proliferation and invasion link biological aggressiveness assessed by MRI with hypoxia assessed by FMISO-PET in newly diagnosed glioblastomas *Cancer Res* **69** 4502-9

Söderberg M, Engeland U, Mattsson S, Ebel G and Leide-Svegborn S 2011 Initial tests of a new phantom for investigation of spatial resolution, partial volume effect and detectability in nuclear medicine tomography. *Journal of Physics: Conference series* **317**

Söderberg M, Mattsson S, Oddstig J, Uusijarvi-Lizana H, Valind S, Thorsson O, Garpered S, Prautzsch T, Tischenko O and Leide-Svegborn S 2012 Evaluation of image reconstruction methods for (123)I-MIBG-SPECT: a rank-order study *Acta radiol* **53** 778-84

Thomas S R, Maxon H R and Kereiakes J G 1976 In vivo quantitation of lesion radioactivity using external counting methods *Med Phys* **03** 253-5

Turkington T, Degrado T and Sampson W 2001 Small spheres for lesion detection phantoms. In: *IEEE Nuclear Science Symp. Conf. Record,* pp 2234-7

Wacker L, Bonani G, Friedrich M, Hajdas I, Kromer B, Nemec M, Ruff' M, Suter M, Synal H A and Vockenhuber C 2010 Micadas: Routine and High-Precision Radiocarbon Dating *Radiocarbon* **52** 252-62

van Dalen J A, Hoffmann A L, Dicken V, Vogel W V, Wiering B, Ruers T J, Karssemeijer N and Oyen W J G 2007 A novel iterative method for lesion delineation and volumetric quantification with FDG PET *Nucl Med Commun* **28** 485-93

Van de Wiele C, Dumont F, Dierckx R A, Peers S H, Thornback J R, Slegers G and Thierens H 2001 Biodistribution and dosimetry of (99m)Tc-RP527, a gastrin-releasing peptide (GRP) agonist for the visualization of GRP receptor-expressing malignancies *J Nucl Med* **42** 1722-7

Van Dort M E, Rehemtulla A and Ross B D 2008 PET and SPECT Imaging of Tumor Biology: New Approaches towards Oncology Drug Discovery and Development *Current computer-aided drug design* **4** 46-53

Wang W, Lee N Y, Georgi J C, Narayanan M, Guillem J, Schoder H and Humm J L 2010 Pharmacokinetic analysis of hypoxia (18)F-fluoromisonidazole dynamic PET in head and neck cancer *J Nucl Med* **51** 37-45

Vesselle H, Schmidt R A, Pugsley J M, Li M, Kohlmyer S G, Vallires E and Wood D E 2000 Lung cancer proliferation correlates with [F-18]fluorodeoxyglucose uptake by positron emission tomography *Clin Cancer Res* **6** 3837-44

Wilding I R and Bell J A 2005 Improved early clinical development through human microdosing studies *Drug Discov Today* **10** 890-4

Vogel J S 1992 Rapid production of graphite without contamination for biomedical AMS *Radiocarbon* **34** 344-50

Vogel J S, Southon J R, Nelson D E and Brown T A 1984 Performance of catalytically condensed carbon for use in accelerator mass spectrometry *Nuclear Instruments and Methods in Physics Research B* 289-93

Xu X M, Trumbore S E, Zheng S H, Southon J R, McDuffee K E, Luttgen M and Liu J C 2007 Modifying a sealed tube zinc reduction method for preparation of AMS graphite targets: Reducing background and attaining high precision *Nucl Instrum Meth B* **259** 320-9

Zankl M and Petoussi-Henss N 2002 Conversion coefficients based on the VIP-Man anatomical model for photons *Health Phys* **82** 254-6